Università degli Studi di Ferrara

DOTTORATO DI RICERCA IN
"MEDICINA MOLECOLARE E FARMACOLOGIA"

CICLO XXXI

COORDINATRICE/COORDINATORE Prof. Di Virgilio Francesco

Investigating Kainate Receptor as a potential target for neuroprotective therapy in *PARK2*-associated Parkinson's Disease

Settore Scientifico Disciplinare BIO/14-Farmacologia

Dottoranda
Dott. Sassone Jenny

(firma)

Tutore
Prof. Morari Michele

(firma)

Anni 2017/2018

INDEX

SUMMARY

Loss of function mutations in the *parkin* gene (*PRKN, PARK2*), which encodes the protein parkin, cause autosomal recessive juvenile parkinsonism (ARJP), a neurodegenerative disease characterized by degeneration of the dopaminergic neurons localized in the substantia nigra pars compacta. No therapy is effective in slowing disease progression mostly because the pathogenesis of the disease is yet to be understood.

Kainate Receptors (KARs) are ionotropic glutamate receptors located at both pre- and postsynaptic membranes in the central nervous system (CNS) where they contribute to excitatory synaptic transmission regulating post-synaptic currents, neurotransmitter release and neuronal excitability. Our previous study showed that KARs are regulated by parkin. We found that parkin interacts with the GluK2 subunit of KARs and that the loss of parkin function or the expression of parkin mutants associated with ARJP lead to GluK2/KAR accumulation and increase of postsynaptic KAR currents in neurons. Because KARs regulate neuron excitability, we hypothesized that KARs accumulation at the post-synapse of ARJP DA neurons dysregulates DA neuron excitability thus leading to DA neuron death.

In this project, we tested the hypothesis that the partial or total block of KAR provides neuroprotective effect in the parkinQ311X mouse model, a transgenic mouse that expresses a human ARJP parkin variant in DA neurons. KAR blockade in parkinQ311X mice was achieved through both a genetic and a pharmacological approach. We tested whether hemizygousity or deletion of the key KAR subunit GluK2 have neuroprotective effects on SNc DA neurons of parkinQ311X mice as quantified by DA neuron firing, and whether the KAR antagonist UBP310 rescues DA neuron dysfunction and death in parkinQ311X.

The results of this study support KAR as a potential target in the neuroprotective therapy of Parkinson’s Disease.

INTRODUCTION

1. INTRODUCTION

1.1. AUTOSOMAL RECESSIVE JUVENILE PARKINSONISM

1.1.1. Clinical features

Mutations in the *PARK2-Parkin* gene (PRKN, OMIM 600116) cause the most common form of Autosomal Recessive Juvenile Parkinsonism (ARJP) typically characterized by young onset, slow clinical course, good response to levodopa and frequent treatment-induced dyskinesias. Until now, 958 *Parkin* mutation carriers (56% men) originated from 663 families have been described. The median age at onset is 31 years; 62% of patients show onset between 20-40 years, 22% of them after 40 years, and 16% before 20 years of age (juvenile form)[1]. *Parkin*-associated early-onset PD is distinct from idiopathic PD (iPD). Recent reviews in the clinical literature on genetic PD have pointed to the lack of detailed description of individual phenotypic features[1,2]. Evidence suggests, however, that, differently from patients with iPD, Parkin patients display dystonia at early disease stages and dyskinesia at exceedingly low dosages of levodopa. Usually independent of levodopa intake, dystonia is described as the presenting symptom in a large percentage of Parkin patients in whom it can be present in isolation for years before the appearance of parkinsonism[3].

In addition to dystonia, parkin patients show dyskinesia at exceedingly low dosages of levodopa as compared to patients with iPD. On the average, the response to low doses of levodopa is reported as being excellent and sustained. However, the likelihood of developing levodopa-induced dyskinesias (LID) is reportedly higher than in individuals with parkinsonism resulting from other aetiologies [4]. Indeed, in some cases LID is induced by very-low-dose levodopa[3].

Clinically, patients with Parkin mutations also show slow disease progression[5]. Other features include early instability, freezing, festination or retropulsion, autonomic dysfunction and brisk reflexes[5]. Patients with Parkin mutations also show sleep benefit, a phenomena described as good mobility upon awaking in the morning.

1.1.2. Genetic features

Parkin gene is localized on chromosome 6q26. It is an extremely large gene (1.4 Mb), consisting of 12 exons and 11 introns with unusually large size (as large as 200 kb). The Parkin protein is synthesized (translated) from the 2.96 kb-RNA transcripts and is composed of four major domains: UBL (ubiquitin-like domain), RING1 (RING-finger domain 1), IBR (In between RING domains) and RING2 (RING-finger domain 2). *Parkin* mutations account for ~50% of ARJP familial cases, for ~70% of sporadic cases with age of onset <20 years and for 2 to 18% of sporadic young onset cases (<45 years old) depending on ethnicity of the study populations[1]. To date, 183 different parkin mutations have been reported: 110 small mutations including 75 missense mutations, 11 nonsense mutations, 17 small deletions, and 7 insertions; 58 exon rearrangements including 35 deletions and 23 multiplications; and 15 intronic changes affecting splicing [6]. Exon rearrangements are the most common alteration with 63% of all index cases carrying at least one exon deletion or multiplication. The most frequent mutation type was found to be DelEx3, a deletion mutation of exon 3. There are some other deletion mutations (exon 2, exon 3−4, exon 4, exon 5, exon 6, exon 7 and exon 8) but they occur at much lower frequencies than DelEx3[7]. The second most frequent mutation was found to be p.Arg275Trp, a missense mutation by which Arg at amino acid residue 275 within the exon 7 is changed to Trp. There are several other point mutations, but at much lower frequencies[7]. A summary of all reported mutations is provided in **Figure 1**.

Overall, a wide range of mutations in Parkin associates with the disease. In most cases there are homozygous or compound heterozygous deletions or mutations leading to complete loss of parkin protein expression in the brains of patients. This finding supports the concept of loss-of-function as the predominant patho-mechanism in PARK2-related parkinsonism[6,7].

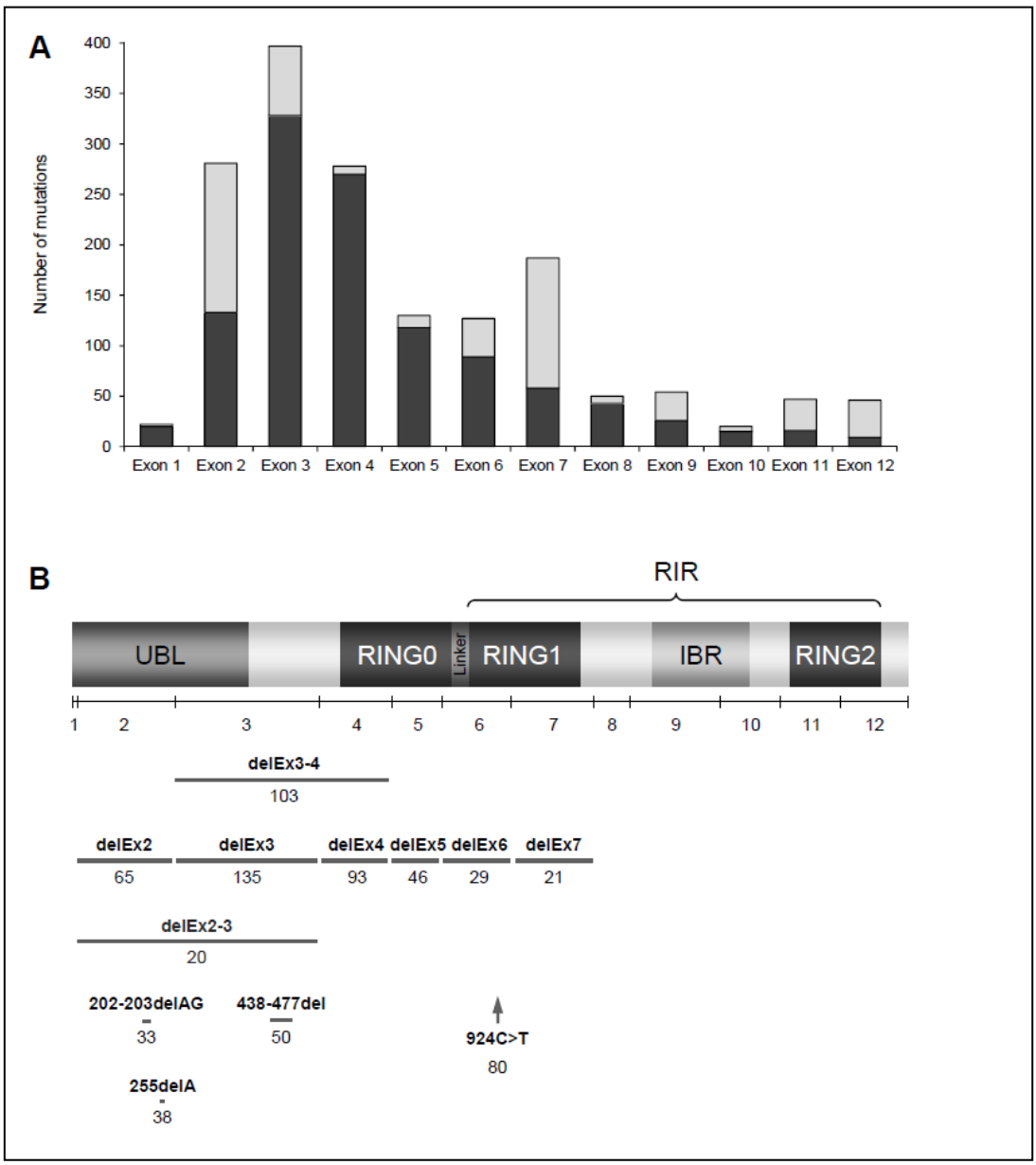

Figure 1. Number and localization of Parkin mutations. (A) Number of Parkin mutations affecting exons 1 to 12. Small mutations are shown in light gray and exon rearrangements in dark gray. (B) Scheme of the domain structure of Parkin showing the localization of mutations with n≥20. Modified from Grunewald et al., 2013.

1.1.3. Neuropathology

Parkin-associated ARJP is characterized by loss of dopaminergic (DA) neurons of the substantia nigra (SN)[8]. There are nine autopsy reports of patients with homozygous or compound heterozygous Parkin mutations[9]. Unlike iPD, neuronal loss is greater in the SN pars compacta (SNpc) than in the locus coeruleus in most parkin cases. The majority of the Parkin autopsies are not associated with alpha-synuclein neuronal inclusions, but some cases had Lewy body (LB) pathology and tau inclusions[9]. Table 1 display a summary of Parkin autopsy reports.

Report	Autopsies	Genotype	Phenotype	Pattern of Neuronal Loss	LB, LN Pathology	LB Distribution—Braak Stage	Tau Pathology—NFT Stage	Other Inclusions
Yamamura et al., 1998	1	Homozygous del between exon 3 and 7	EOPD	SNpc>LC	—	—	—	—
Mori et al., 1998	1	Homozygous exon 4 del	EOPD	SNpc>LC	—	—	III	Thorn-shaped astrocytes
Hayashi et al., 2000	1	Homozygous exon 4 del	EOPD	SNpc>SNpr, LC	—	—	Sparse	
van de Warrenburg et al., 2001	1	Compound heterozygous exon 3 del/exon 6 transversion	EOPD	SNpc>LC	—	—	—	Thorn-shaped astrocytes
Mori et al., 2003	1	Compound heterozygous exon 6del/exon 7 del	EOPD	SNpc>LC	—	—	—	—
Gouider-Khouja et al., 2003	1	Homozygous exon 2 del	EOPD	SNpc, SNpr>LC	—	—	—	—
Farrer et al., 2001	1	Compound heterozygous exon 7 R275W/exon 3 del	EOPD, writer's cramp	SNpc, LC	+	4	—	—
Pramstaller et al., 2005	1	Compound heterozygous exon 7 del and 1072T del	PD	SNpc, LC	+	3	—	—
Sasaki et al., 2004, 2008	1	Homozygous exon 3 del	EOPD	SNpc>LC	Basophilic LB-like in PPN	—	—	Eosinophilic LB in anterior horn cells
Morales et al., 2002	1	Heterozygous C212Y mutation	PSP	SNpc/pr, striatum, GP, nbM, STN, thalamus	—	—	—	PSP

Table 1. Summary of *Parkin* Autopsy Reports Abbreviations: del, deletion; SNpr, substantia nigra pars reticulata; GP, globus pallidus. Modified from Poulopoulos et al., 2018.

1.1.4. The protein parkin

Parkin is a ubiquitin-ligase enzyme expressed in the central nervous system (CNS) and in peripheral tissues[10–15]. At the intracellular level, it catalyzes the transfer of ubiquitin from ubiquitin-carrier enzymes to protein substrates and regulates their trafficking and turnover[16–18]. Numerous substrates for parkin have been identified, indicating that it is a multifunctional protein involved in many intracellular processes, including the control of mitochondrial integrity and the regulation of apoptosis and transcription[19,20]. Parkin consists of a ubiquitin-like domain (Ubl) at its N terminus and four zinc-coordinating RING-like domains: RING0, RING1, IBR and RING2. The Ubl domain is involved in substrate recognition, binding SH3 and ubiquitin interacting motif (UIM) domains, proteasome association and regulation of cellular parkin levels and activity. Domains RING0 through RING2 (collectively referred to as R0–RBR) each coordinate two zinc ions through histidine and cysteine residues, confirming the stoichiometry of eight zinc ions per parkin molecule. The IBR domain is conserved among the RBR E3 family; the precise function of the domains is currently unknown[21].

The activity of parkin is tightly controlled by multiple mechanisms of autoinhibition. The first is access to the catalytic RING2 domain, which is blocked by RING0. A second mechanism is the control of binding of the upstream E2 enzyme to parkin. Modeling and mutagenesis have confirmed that the E2 binding site is on the RING1 domain, but the site is occluded by the Ubl domain and REP linker. Finally, the large distance between the E2 binding site and the catalytic site on RING2 prevents transfer of ubiquitin from the ubiquitin–E2 conjugate to the parkin catalytic cysteine[21].

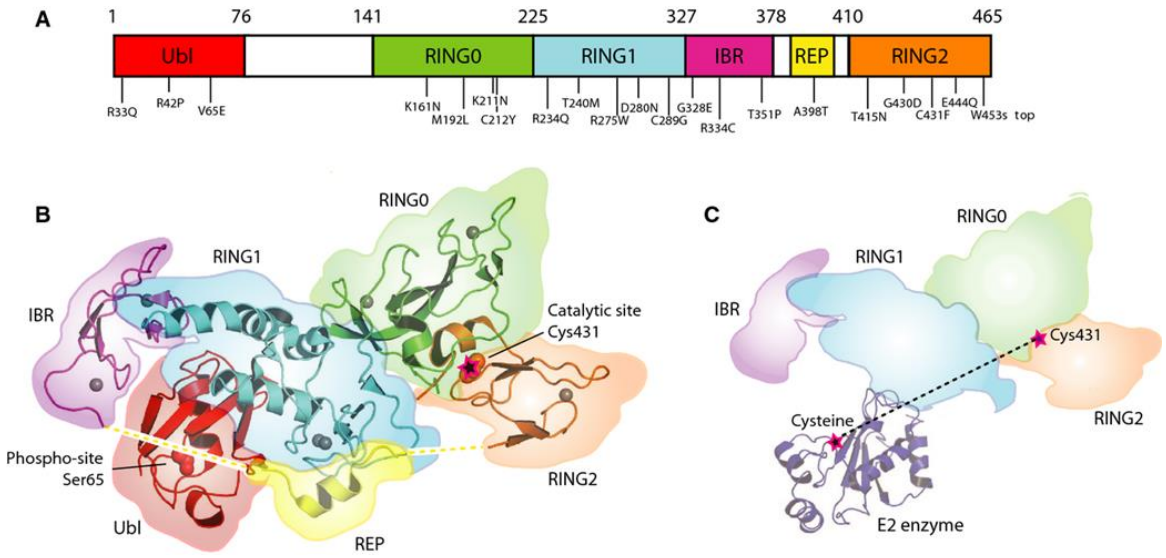

Figure 2. (A) Domain architecture of the five parkin domains and identification of selected PD mutations. (B) Cartoon representation of parkin. Parkin activity depends on two functional sites: a binding site for ubiquitin-conjugated E2 enzyme on the RING1 of parkin, and a catalytic site with a cysteine that forms a transient covalent linkage with ubiquitin on the RING2 domain. Both sites are occluded in the autoinhibited structure. The Ubl domain and REP linker between the IBR and RING2 domains prevent the E2 from binding to RING1. The RING0 domain partially covers the catalytic cysteine on the RING2 domain. The eight structural zinc ions in parkin are shown as gray spheres. Dashed lines indicate portions of the IBR and RING2 linker that were not observed in the crystal structure. (C) Model of an E2 enzyme bound to parkin with Ubl and REP linker removed. An additional structural rearrangement must occur to allow ubiquitin on the E2 enzyme to transfer to the catalytic cysteine of parkin. The E2 and parkin catalytic cysteines are ~50 Å apart in the model. Modified from Seirafi et al., 2015.

1.2. THE KAINATE RECEPTOR

1.2.1. Structure of KARs

The protein family of ionotropic glutamate receptors (iGluRs) comprises three receptor subfamilies named α-amino-3-hydroxy-5-methylisoxazole-4-propionic acid (AMPA), N-methyl-D-aspartate (NMDA), and kainate (KA) receptors. All iGluRs share a tetrameric subunit composition as well as a common subunit topology in which the N-terminal domain (NTD) is located extracellularly, followed by three transmembrane domains (known as membrane domains M1, M3, and M4), a re-entrant loop (pore loop or M2) penetrating the membrane from its intracellular side between TMDs A and B, and a cytoplasmic C-terminal domain (CTD). KARs are tetrameric receptors composed of various combinations of five GluK1-5 subunits (formerly named GluR5, GluR6, GluR7, KA1 and KA2, respectively). GluK1-3 can form functional homomeric and heteromeric receptor channels and have multiple isoforms derived from alternative splicing and RNA editing. GluK4-5 do not form functional homomeric channels but can co-assemble with GluK1-3 subunits[22]. GluK2 is the key subunit that promotes the cell surface expression of other KAR subunits[23,24]. The structure of KARs and the different subunits are reported in figure 3 and 4.

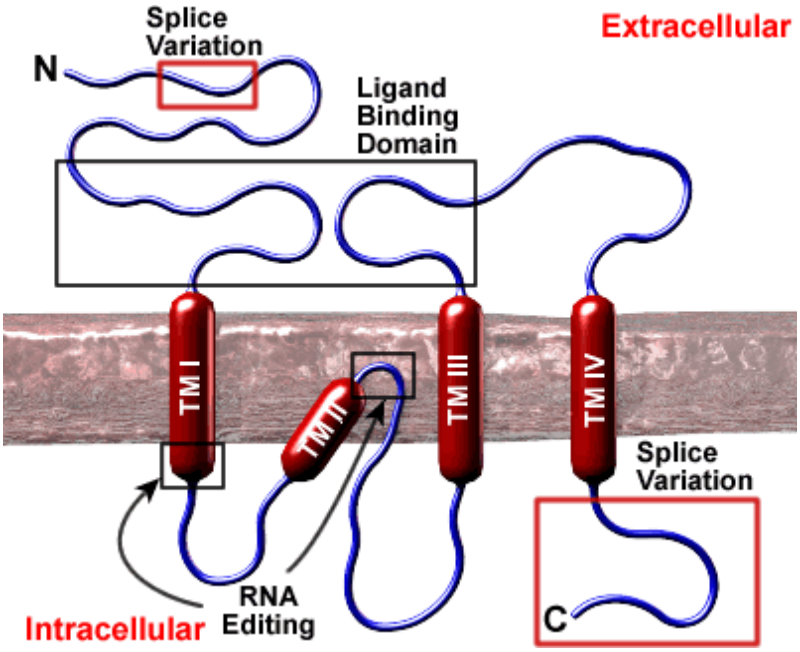

Figure 3. Simplified structure of KAR subunits.

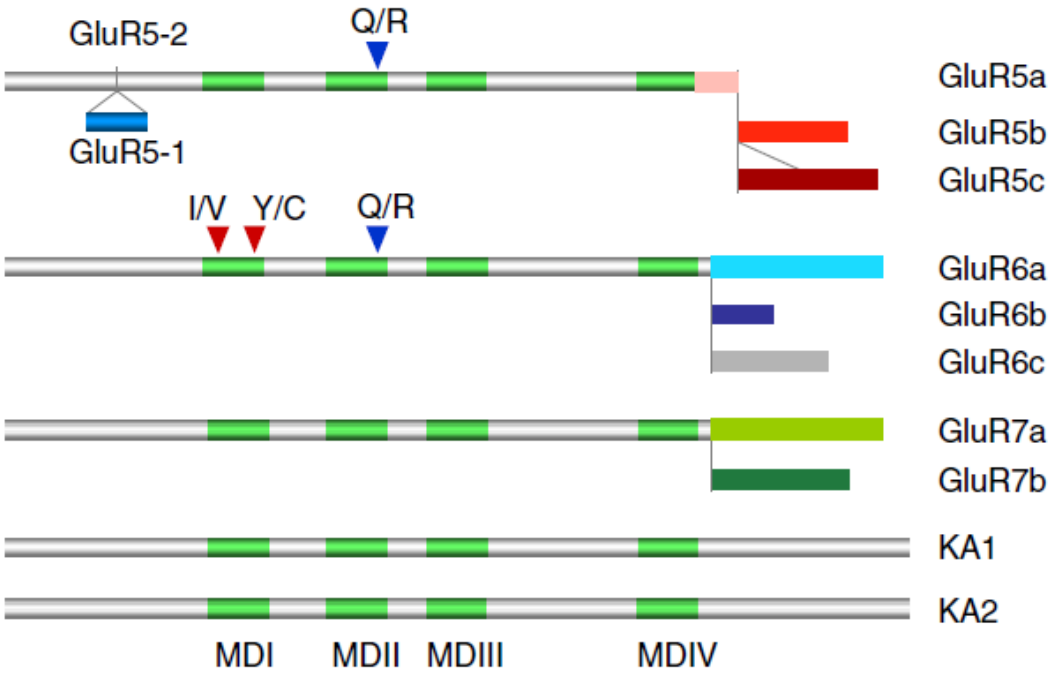

Figure 4. Splice variants of KAR subunits. The membrane domains are in green. GluK1 has two N-terminal splice variants, with a 15 amino acid insertion in GluK1-1 compared with GluK1-2, and three C-terminal splice variants in the cytoplasmic domain. GluK2 and GluK3 each have two splice variants (a and b) in their C-terminal cytoplasmic domains. No splice variants for GluK4 and GluK5 have been found. Modified from Coussen 2009.

1.2.2. Localization of KAR in the brain

The distribution of the KAR subunit mRNAs have been investigated both in rodent and in the human brain and results have shown many similarities and some differences[25]. In a study aimed at investigating KAR expression in hippocampus, neocortex and cerebellum in the human brain, GluK1 (GluR5) mRNA was detected only in Purkinje cells and a few scattered hippocampal neurons. GluK2 (GluR6) mRNA was relatively abundant in all areas, notably in dentate gyrus, pyramidal neurons of CA3, and cerebellar granule cells, and detectable in superficial and deep laminae of the neocortex. Moderate signal for GluK3 (GluR7) mRNA was seen in deep laminae of the neocortex while a weak signal in the dentate gyrus; GluK3 mRNA was also apparent over some

pyramidal and non-pyramidal cells in hippocampus and over putative cerebellar stellate/basket cells. GluK4 mRNA was detected only in the dentate gyrus. The expression profile of GluK5 (KA2) mRNA was similar to that of GluK2 (GluR6) mRNA. Hybridization of rat brain sections indicated that the regional and cellular distribution of KA receptor subunit mRNAs in human hippocampus, neocortex and cerebellum largely parallels that in the corresponding areas of rat brain, albeit at lower levels, especially with regard to GluK1 (GluR5) and GluK4 (KA1) transcripts (Table 2)[25].

mRNA	Human								Rat							
	Hippocampus			Cortex		Cerebellum			Hippocampus			Cortex		Cerebellum		
	DG	CA3	CA1	Sup	Deep	GC	PjC	S/BC	DG	CA3	CA1	Sup	Deep	GC	PjC	S/BC
GluR5	–	–	–	–	–	–	++	–	++	+	+	+	+	nd	nd	nd
GluR6	+++	+++	+	++	++	+++	–	–	+++	+++	+	++	++	+++	–	–
GluR7	+	+	–	+	++	–	+	+	+++	+	+	++	+++	nd	nd	nd
KA1	+	–	–	–	–	–	–	–	+	+++	+	+	+	nd	nd	nd
KA2	+++	+++	+	++	++	++	–	–	+++	+++	+++	+++	+++	+++	–	–

Table 2. Distribution of KAR subunit mRNA in selected areas of human and rat brain. -: no consistent labelling; +: weak signal; ++: moderate signal; +++: strong signal; nd: not determined. Ratings in hippocampus and cortex are determined from film autoradiography; cerebellar ratings based upon dipped sections. Abbreviations: DG, dentate gyrus. Sup, superficial laminae. Deep, deep laminae. GC, granule cell layer. PjC, Purkinje cells. SrBC, stellate/basket cells. Modified from Porter et al., 1997.

The expression of KAR subunits was also investigated in DA neurons. The transcripts encoding all five KAR subunits were found in the human SNc: the GluK2 subunit was the most abundant kainate receptor subunit, although levels of expression for GluK1 and GluK5 subunits were also high[26]. More recently, the UK Brain Expression Consortium made available the results of a gene expression study in multiple regions from human brains. Figure 5 displays the expression levels of genes GRIK1-5 encoding for KAR subunits GluK1-5 in human brain tissues. Data derive from Central Nervous System tissues originating from autopsy of 134 control individuals. These results further confirm that KAR subunits are expressed in DA neurons of SNc.

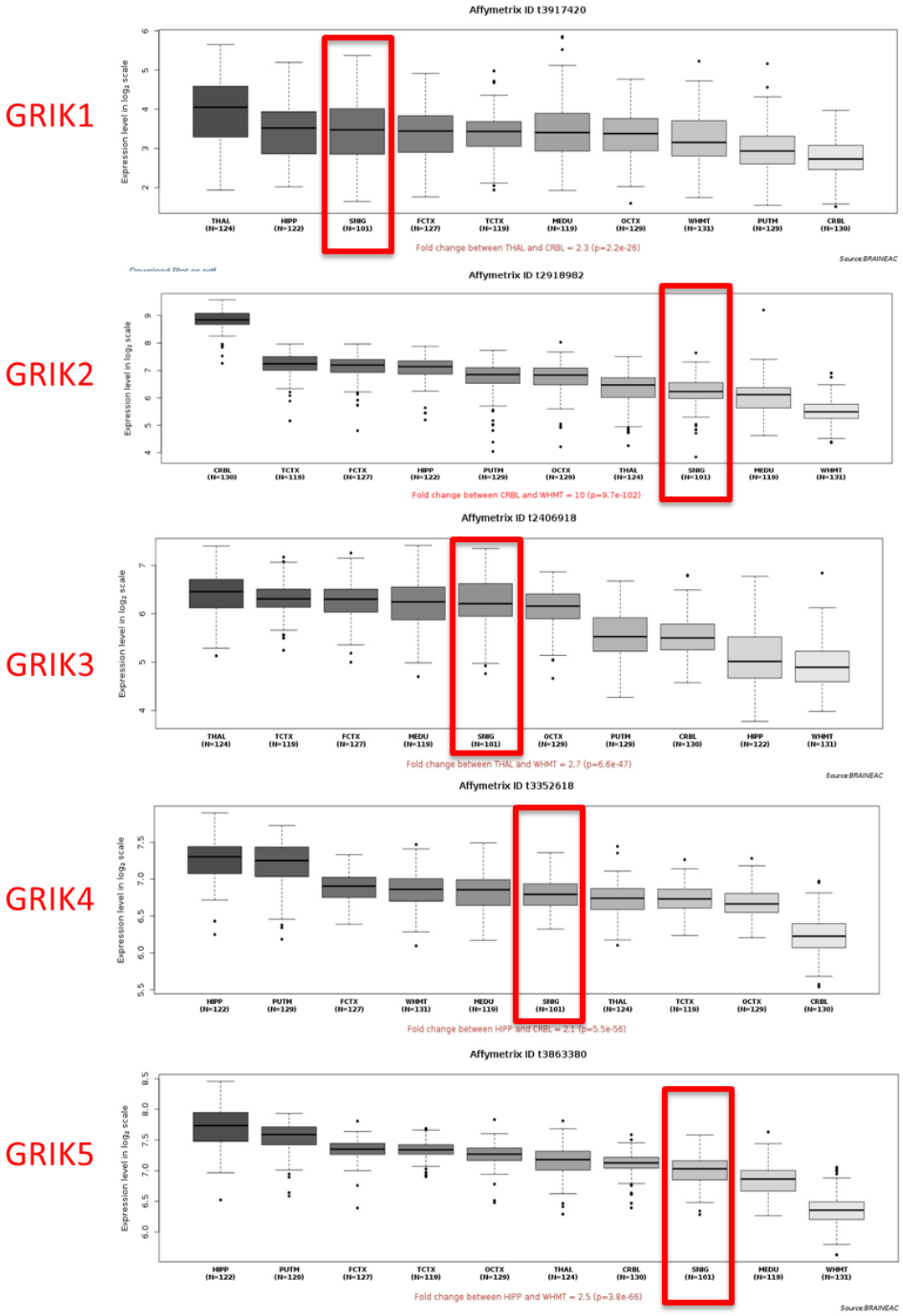

Figure 5. Expression levels of genes GRIK1-2-3-4-5 encoding for KAR subunits GluK1-2-3-4-5 in human brain tissues. Data derive from Central Nervous System tissues originating from autopsy of 134 control individuals. All individuals were confirmed to be neuropathologically normal. From each individual 10 brain regions were analyzed: cerebellar cortex (CRBL), frontal cortex (FCTX), hippocampus (HIPP), medulla (specifically inferior olivary nucleus, MEDU), occipital cortex (specifically primary visual cortex, OCTX), putamen (PUTM), substantia nigra (SNIG), thalamus (THAL), temporal cortex (TCTX) and intralobular white matter (WHMT). RNAs were isolated and samples analyzed using Affymetrix Exon 1.0 ST Arrays. Data derive from UK Brain Expression Consortium (UKBEC) http://www.braineac.org/

Although all the ionotropic glutamate receptors are ligand-gated ion channels, they serve distinct functions within the CNS. KARs comprise the probably least understood group of iGluRs. A comprehensive analysis of the controversial literature on KARs allows to conclude that these receptors play significant roles in the brain at three main levels. At the postsynaptic level, KARs contribute to the synaptic response, mediate postsynaptic depolarization and are responsible for carrying some of the synaptic current at some synapses. Unlike AMPAR-mediated currents, the activation of postsynaptic KARs by endogenous glutamate yields small amplitude excitatory postsynaptic currents (EPSCs), with slow activation and deactivation kinetics[27]. KARs are also present at presynaptic locations, where they regulate transmitter release at both excitatory and inhibitory synapses (glutamate and GABA, respectively). Third, they play an influential role in the maturation of neural circuits during development [27]. Intriguingly, KARs mediate two forms of signaling, a canonical pathway involving ion flux and another, non-canonical signaling pathway which links KAR activation to G protein activation. The gating of the channel (canonical pathway) is responsible for membrane depolarization, the synaptic responses and, probably, for the facilitation of neurotransmitter release at some synapses. On the other hand, KARs activate G proteins signaling through the stimulation of phospholipase C and PKC in a manner independent of ion flux (non-canonical pathway). It is unknown whether these receptors require an intermediate protein to couple to G protein[27,28].

1.3. THE POTENTIAL ROLE OF PARKIN AT THE SYNAPSE

Studies conducted over the last 15 years point to an important role of parkin in modulating neurotransmission. Collectively, these findings supports the role of parkin in modulating synapse functions and highlight that *parkin* gene mutations found in ARJP patients may cause dysregulation of the glutamatergic and dopaminergic synapses that culminates in dopaminergic neuron dysfunction and death.

1.3.1. Parkin localizes to presynaptic and postsynaptic terminals

Parkin is a cytosolic protein diffusely distributed in neuronal axons, soma, and dendrites[29]. Preliminary investigations disclosed that parkin is localized at synaptic vesicles and displays a distribution pattern similar to that of synapsin I (antibody M74)[30], a protein that associates with the cytoplasmic surface of synaptic vesicles[31]. An immunoelectron microscopy study, performed with the ASP5p antibody, not yet validated using tissues from parkin-knockout mice, showed that parkin is not localized within the vesicles, but rather in direct juxtaposition to their membranes[32]. This study showed that parkin also localizes at the postsynaptic density (PSD) (antibody ASP5p). Consistently, differential fractioning of rat brain lysates revealed that parkin was enriched in the fraction containing PSD-95 (antibody ASP5p)[33], the prototypic PSD marker[34]. An immunoelectron microscopy study also showed that the parkin staining intensity was higher in the postsynaptic than in the presynaptic elements (antibody ASP5p).

Although evidence for the specificity of parkin antibodies in immunohistochemistry experiments is limited, these results show that parkin localizes to presynaptic terminals, where it associates with synaptic vesicles, and at postsynaptic terminals, where it associates with PSDs. These subcellular localization data are consistent with the hypothesis that parkin regulates synaptic functions.

1.3.2. The role of parkin at the excitatory synapse: parkin interacts with and ubiquitinates proteins of the postsynaptic densities

The postsynaptic compartment detects the neurotransmitters released from the presynaptic terminal and transduces this signal into electrical and biochemical changes in the postsynaptic cell. In excitatory neurons, the postsynaptic compartment includes the PSD, whose spatial organization is orchestrated by scaffold proteins containing protein-protein interaction modules of 80-90 amino acids, termed postsynaptic density-95, disc large, zona occludens (PDZ) domains[35]. The extreme C-terminus of parkin contains a potential PDZ binding motif[33]. This evidence led to the hypothesis that parkin can interact with and/or ubiquitinate PSD proteins, modulating their localization and turnover. Indeed, parkin was found to interact with PSD-95[33], which is the best characterized PSD scaffold protein of the excitatory synapses. PSD-95 is involved in anchoring synaptic proteins, including NMDA receptors (NMDAR), AMPA and KA receptors (AMPA/KAR), and K^+ channels[34], modulating their levels at the cell surface, and linking these postsynaptic receptors with their downstream signaling proteins. Because of the key role that PSD-95 plays in modulating membrane receptor levels and functions, the interaction between parkin and PSD-95 suggests that parkin regulates the trafficking, anchoring and clustering of membrane receptors. Parkin was also found to interact with the synaptic scaffolding molecule CASK (Ca^{2+}/CaM-associated serine kinase)[33] that has a key role in maintaining the morphology of dendritic spines[36].

Besides these parkin-interactors, several other substrates of parkin ubiquitination have been identified within the PSD. Parkin monoubiquitinates PICK1, a synaptic scaffold protein that controls the trafficking of numerous neurotransmitter receptors, transporters, ion channels and enzymes[37]. This monoubiquitination appears to regulate the effects of PICK1 on the acid-sensing ion channel ASIC2a. Given that ASIC channels contribute to excitotoxicity, it has been posited that loss of parkin may enhance ASIC activity and thereby promote neurodegeneration[37].

To further investigate the role of parkin at the excitatory synapse, we completed a study to determine whether parkin interacts with ionotropic glutamate receptors. We found that parkin interacts with and ubiquitinates the GluK2 subunits of KAR, and thus regulates KAR currents[38]. The observation that parkin affects somatodendritic KAR currents is consistent with the idea that parkin-GluK2 interaction takes place at postsynaptic sites. Since parkin is

localized in axons as well, we cannot exclude the possibility that it also regulates presynaptic GluK2-containing KARs, which are involved in facilitating synaptic transmission.

A more recent study on neurotransmitter receptor levels in parkin-knockout mice confirmed the upregulation of KAR densities in numerous cortical areas of parkin-knockout mice. It was also found that NMDAR levels were increased and AMPAR densities were decreased in different brain regions of parkin-knockout mice[39]. The alterations of three different glutamate receptor types underline the potential relevance of the glutamatergic system in the pathogenesis of *parkin*-related PD. Overall, these findings, mainly obtained on cortical or hippocampal preparations, indicate that parkin interacts with and ubiquitinates proteins located at the excitatory synapse both pre- and postsynaptically (Fig. 1 and Table 1). This evidence suggests that parkin orchestrates a general as yet uncharacterized remodeling of synaptic function.

1.3.3. Parkin modulates excitatory synaptic transmission: the excitotoxicity hypothesis

SNc neurons receive glutamatergic inputs from various brain areas, including the cortex, pedunculopontine nuclei, superior colliculus, thalamus and subthalamic nucleus[40]. While these glutamatergic inputs are essential for basal ganglia physiology, excessively high levels of extracellular glutamate can lead to hyperactivation of ionotropic glutamatergic receptors localized on the dopaminergic neuron membrane and trigger a cascade of intracellular events that promote dopaminergic neuron death. The ensemble of these glutamate-triggered events, termed excitotoxicity, has long been hypothesized to have a key role in PD pathophysiology[41,42]. In addition to causing primary damage, excitotoxicity may also contribute to PD progression, since DA deficiency causes the STN to display a continuous abnormal “bursting” mode of activity[43] that releases high amounts of glutamate in the SNc, which can further exacerbate excitotoxic injury[44,45]. Given the role parkin may play in modulating excitatory synapse functions, the “excitotoxicity” hypothesis, initially formulated to explain the aetiology of sporadic PD, fits perfectly with the known causes of ARJP. Loss of parkin function may result in primary excitotoxic damage through the upregulation of glutamate receptors. This hypothesis is supported by

experimental evidence. The postsynaptic expression of ARJP parkin variants results in pruning of excitatory synapses and increased amplitudes of miniature excitatory postsynaptic currents[29]. Since such currents are the postsynaptic response to the release of a quantum of neurotransmitter from a single synaptic vesicle[46,47], glutamatergic neurotransmission is increased in ARJP neurons. ARJP neurons are also more vulnerable than control neurons to excitotoxic stimuli[29]. The observed increase in neurotransmission is consistent with higher density/conductance of glutamatergic postsynaptic receptors at individual synapses and suggests that a loss of parkin function increases the density/conductance of postsynaptic receptors.

The postsynaptic currents at the excitatory synapses of dopaminergic neurons consist of two components: a rapid component mediated by AMPAR/KAR and a slower component mediated by NMDAR[48]. Evidence suggests that, among ionotropic glutamate receptors potentially involved in excitotoxicity, parkin directly regulates AMPAR/KAR. Interestingly, upon silencing of endogenous parkin, dopaminergic neurons are more vulnerable than control neurons to treatment with kainate, an AMPAR/KAR agonist, and this effect is rescued by overexpression of wild-type parkin[49]. In line with these observations, loss of parkin function was demonstrated to potentiate KAR currents and increase KAR-dependent excitotoxicity[38].

Overall, accruing evidence suggests that parkin modulates the density/conductance of glutamate postsynaptic receptors and that loss of parkin upregulates excitatory currents, leading to dopaminergic neurons death by excitotoxicity. Moreover, because DA deficiency induces STN hyperactivity that, in turn, increases glutamate release in the SNc [43,45,50], we can hypothesize that parkin loss of function in ARJP patients may cause primary excitotoxic damage that precedes the excitotoxic damage due to overactivity of the STN glutamatergic neurons.

2. AIM OF THE PROJECT

Since previous study showed that parkin, the protein causative of ARJP, regulates KARs, and that *PARK2* mutations increase KAR levels/currents in neurons, we hypothesized that KARs accumulation at the post-synapse of ARJP DA neurons dysregulates DA neurons excitability, thus leading to DA neurons death. This project tested the hypothesis that genetic or pharmacologic block of KAR provides neuroprotective effect in the ARJP mouse model, parkinQ311X. ParkinQ311X is a transgenic mouse that expresses a human ARJP parkin variant in DA neurons[51]. This model has been selected for this study because it recapitulates SNc degeneration typical of ARJP. This study aims at enhancing existing data supporting KAR as potential target in neuroprotective therapy of ARJP or refuting validity of this target to treat ARJP.

MATERIALS AND METHODS

3. MATERIALS AND METHODS

3.1. Animal models

For this study, we used two different mouse strains: C57B1/6N ParkinQ311X and C57B1/6N GluK2 knock-out. The C57B1/6N ParkinQ311X mouse was previously generated and characterized[51]. Briefly, a FLAG-tagged human mutant parkin carrying the Q311X mutation followed by a polyadenylation signal, was inserted into exon 2 of the Slc6a3 gene preceding the endogenous translation initiation codon. Hemizygous ParkinQ311X mice are viable and fertile, with expression of a FLAG-tagged, C-terminal truncated human parkin-Q311X mutation associated with Turkish early-onset PD[52] directed to dopaminergic neurons of the substantia nigra pars compacta (SNc) and ventral tegmental area (VTA) by the mouse Slc6a3 promoter/enhancer sequences. ParkinQ311X mice express the FLAG-tagged parkin-Q311X protein in dopaminergic neurons at a level that is approximately equivalent to or just below that expected from a heterozygous endogenous parkin allele. Genotyping of this mouse colony for this study was performed according to the previously published protocol[51].

C57B1/6N GluK2 knock-out mice were generated in a previous study by disrupting the Grik2 gene by homologous recombination[53]. Genotyping of this mouse colony for this study was performed according to the original protocol[53].

Mice were maintained and bred at the animal house of Ospedale San Raffaele in compliance with institutional guidelines and international laws (EU Directive 2010/63/EU EEC Council Directive 86/609, OJL 358, 1, December 12, 1987, NIH Guide for the Care and Use of Laboratory Animals, U.S. National Research Council, 1996). The experiments were planned and conducted with the aim of minimizing the number of sacrificed animals.

3.2. Cell-attached and whole-cell patch clamp recordings in DA neurons of the SNc in mouse brain slices

Twenty-five (25) days-old mice were anesthetized by intraperitoneal injection of a mixture of ketamine/xylazine and perfused transcardially with ice-cold artificial cerebrospinal fluid (ACSF) saturated with 95% O_2 and 5% CO_2 (pH 7.3). After decapitation, the brains were removed from the skull and 300 µm-thick parasagittal

cortico-striatal slices were cut in ACSF at 4°C using a VT1000S vibratome (Leica Microsystems, Wetzlar, Germany). Individual slices were submerged in a recording chamber mounted on the stage of an upright BX51WI microscope (Olympus, Japan) equipped with differential interference contrast optics (DIC). Slices were perfused with ACSF continuously flowing at a rate of 2-3 mL/min at 32°C. DA neurons were analyzed for spontaneous firing frequencies and intrinsic membrane parameters (e.g., action potential amplitude, threshold).

3.3. Stereological cell count in SNc

Animals were deeply anesthetized and transcardially perfused with 0.9% NaCl solution followed by 4% paraformaldehyde in PBS (0.1 M, pH 7.4). Brains were removed, transferred to a 30% sucrose solution in PBS for cryoprotection and stored at −80°C. Coronal sections (40 µM) encompassing the whole SNc (AP from −3.16 to −3.52 from bregma)[54] were cut using a cryostat (Leica Microsystems, Wetzlar, Germany), and then collected free floating for immunohistochemistry. Serum containing TH antibody (polyclonal rabbit primary TH antibody, J. Boy, Reims, France) was diluted 1:2000 in PBS containing 0.3% Triton X-100 and 1% bovine serum albumin (BSA). Sections were incubated overnight at 4°C with primary antibody, then for 1 h with biotinylated horse anti-rabbit antibody (universal secondary antibody, AbCys SA, Paris, France) diluted 1:200 in PBS containing 1% BSA and 0.3% Triton X-100, and finally revealed with 3,3′-diaminobenzidine tetrahydrochloride (DAB kit, Vector Laboratories). Sections were then mounted on gelatine-coated slides, counterstained with cresyl violet, dried with ethanol and xylene and coverslipped with mounting medium. To count TH positive (TH +) neurons (phenotypic marker) and cresyl violet stained cells (structural marker) in SNc, an unbiased stereological sampling method based on optical fractionator stereological probe was used as previously described. TH+ neurons were counted using a Leica DM6000B motorized microscope coupled with the Mercator Pro Software (Mercator Digital Imaging System, Explora Nova, La Rochelle, France). Five sections were used for each brain. For each animal, SNc boundaries were delimited at low magnification (2.5x) by examining the size and shape of the different groups of TH+ neurons and their axonal projections, as well as nearby fiber bundles[54] (Paxinos and Franklin, 2001), and probes for stereology were applied. Any TH+ cell within the probe, or intersecting an acceptance line delimiting the

probe (green line) that came into focus at 40x magnification was counted. The optical fractionator method was then used to estimate the total number of TH+ cells in the SNc of each animal.

3.4. TH quantification in striatum

Coronal sections (35 µm) of striatum (AP from + 1.42 to + 0.14 from bregma) and SNc (AP from −3.16 to −3.52 from bregma)[54] were cut with a cryostat and then collected free floating in five different series for immunohistochemistry. After being rinsed in TBS (Tris Buffered Saline), serial SNc sections were incubated for 1 h with blocking solution (Bovine Serum Albumin; 3% in TBS), then incubated overnight with TH primary antibody (Purified rabbit polyclonal antibody; 1:500 in 1% BSA in TBS; Merck Millipore, Darmstadt, Germany) and with a fluorescent marker of Nissl Bodies (Neurotrace; 1:150 in 1% BSA in TBS; Life Technologies, Grand Island, NY, USA). Sections were then incubated with a secondary antibody (AlexaFluor 488, Goat anti-rabbit IgG; 1:500 in TBS; Life Technologies) for 40 min, mounted on slides and coverslipped with mounting medium. Three representative striatal sections were incubated for 1 h with blocking solution (Goat Serum 5% in TBS), then incubated overnight with TH primary antibody (Purified rabbit polyclonal antibody; 1:500 in 1% Goat Serum in TBS; Merck Millipore, Darmstadt, Germany). Finally, sections were incubated with a secondary antibody (AlexaFluor 488, Goat anti-rabbit IgG; 1:500 in TBS; Life Technologies) for 40 min, mounted on slides and coverslipped with mounting medium. 2.9.1. Images were taken at 20x magnification with NanoZoomer 2.0 HT (BIC facility, Bordeaux), and optical densitometry analyzed off-line as gray level with ImageJ using the cerebral cortex as background.

3.5. Mouse treatment with UBP310 or vehicle

UBP310 was dissolved in 100% DMSO at the concentration of 10 mg/mL and then diluted in 90% Saline + 10% DMSO at 1 mg/mL. Mice were injected i.p. with UBP310 (20mg/Kg) or with an equivalent volume of vehicle.

3.6. Analyses of UBP310 concentration in brain tissues

Brain samples (100 mg) were homogenized in 1 mL of methanol/water 85:15 (v/v), containing 10 ng of IS (tryptophan-D5). Samples were stored for 20 min at -80°C, in

order to allow the separation of fat materials. Homogenates were centrifuged for 15 min at 13.200 rpm at 4°C and 500 µl of the supernatants were dried under nitrogen and re-suspended in 100 µl of chromatographic mobile phase for instrumental analysis. The concentration of UBP310 in brain tissues was analyzed with API 5500 (Sciex): high-performance liquid chromatography coupled to mass spectrometry.

3.7. In-vivo single-unit extracellular recordings of SNc DA neurons

Mice were anaesthetized with chloral hydrate (400 mg/kg, i.p.) and placed in a stereotaxic apparatus. To maintain a full anaesthetic state during the experiments, supplemental doses of chloral hydrate (100 mg/kg, i.p.) were periodically administered. Anaesthesia was confirmed by the absence of nociceptive reflex reaction to a tail or a paw pinch and of an eye blink response to pressure. To perform in-vivo single-unit extracellular recordings of SNc DA neurons, a hole was drilled through the skull and the electrode was lowered slowly.

3.8. Western blot analyses

Brain tissues were homogenized with lysis buffer (20mM Tris, pH 7.5, 150mM NaCl, 1mM EDTA, 1mM EGTA, 1% Triton X-100, protease inhibitors (Roche), 50mM MG132 and 10mM N-ethylmaleimide (Sigma)). Western blottings were performed with Novex NuPAGE SDS–PAGE gels (Invitrogen). The following antibodies were used: GluA2/3 (AB1506, Millipore, 1:1,000), TH (clone LNC1, Millipore), GAPDH (sc-25778, Santa Cruz, 1:1,000).

3.9. Materials

UBP310 was purchased from ABCAM (Cambridge, UK). It was dissolved to 10 mg/mL in 100% DMSO, and the solution diluted in 10% DMSO/saline to 1 mg/mL solution to be injected i.p.

3.10. Data presentation and statistical analysis

Data are presented as mean ± standard error of the mean (SEM). Data were subjected to the normality test (Kolmogorov–Smirnov test) and equal variance test (Bartlett's test). Unpaired Student's t-test, unpaired two-tailed, was used to compare two groups of data. One-way ANOVA followed by appropriate post hoc tests was used to compare multiple groups. Data that did not satisfy the

assumptions of the parametric tests were analyzed using the Kruskal–Wallis test followed by Dunn's multiple comparisons test. The effects of cumulative doses of UBP310 (10-60mg/Kg, i.p.) on SNc DA firing activity was analyzed using one-way ANOVA for repeated measures followed by the Bonferroni post-hoc test for multiple comparisons. The ED50 of UBP310 was calculated via non-linear regression analysis. P-values <0.05 were considered to be statistically significant. Analyses were performed using the GraphPad Prism6 software.

RESULTS

4. RESULTS

4.1. ParkinQ311X mice show early dysfunction and death of SNc DA neurons

Parkin-Q311X is a Bacterial Artificial Chromosome (BAC) transgenic mouse model expressing a C-terminal truncated human mutant parkin in DA neurons under a dopamine transporter promoter (**Figure 6**).

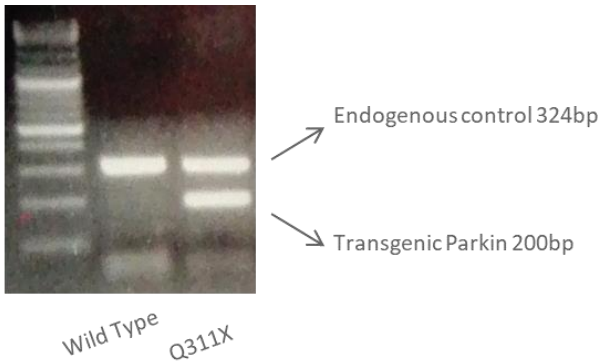

Figure 6. Genotyping of Parkin-Q311X mice. Representative agarose gel showing the ParkinQ311X transgene.

According to the first paper describing this model, Parkin-Q311X mice exhibit DA neuron degeneration in SNc at 16 months of age [51]. However, that study did not investigate whether this mouse develops DA neuron dysfunction and death at earlier time-points. To address this point, we recorded spontaneous firing activity of SNc DA neurons in acute slices of ventral midbrain prepared from 25 days-old mice. We found that spontaneous firing frequency of SNc DA neurons was increased in ParkinQ311X mice compared to WT littermates (**Figure 7**).

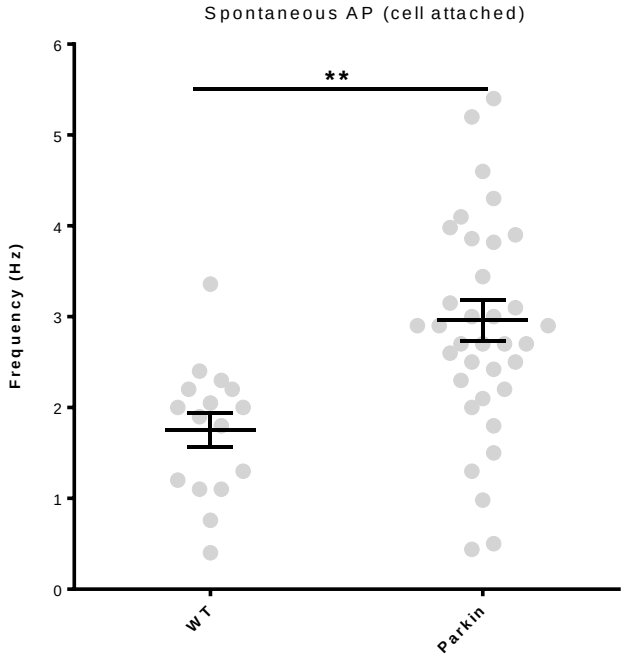

Figure 7. Early dysregulation of SNc DA neuron firing in Parkin-Q311X mice. Representative recordings of the spontaneous firing activity of SNc DA neurons in acute slices of ventral midbrain prepared from mice at 25 days of age. Data derive from 8 ParkinQ311X mice (36 recorded neurons) and 6 WT littermates (16 recorded neurons) (Student's t-test, unpaired two tailed **p<0.001).

To test if Parkin-Q311X mice exhibit early DA neuron degeneration, we performed a stereological count of SNc DA neuron at 6 months of age. Six-month-old mice were deeply anesthetized and transcardially perfused with paraformaldehyde (see Methods). Stereological cell count in SNc and analysis of tyrosine hydroxylase (TH) density in striatum were performed according to standard protocols[55,56]. Results of stereological cell count in SNc are reported in **figure 8**. ParkinQ311X mice showed a reduced number of DA neurons in SNc as compared to WT littermates.

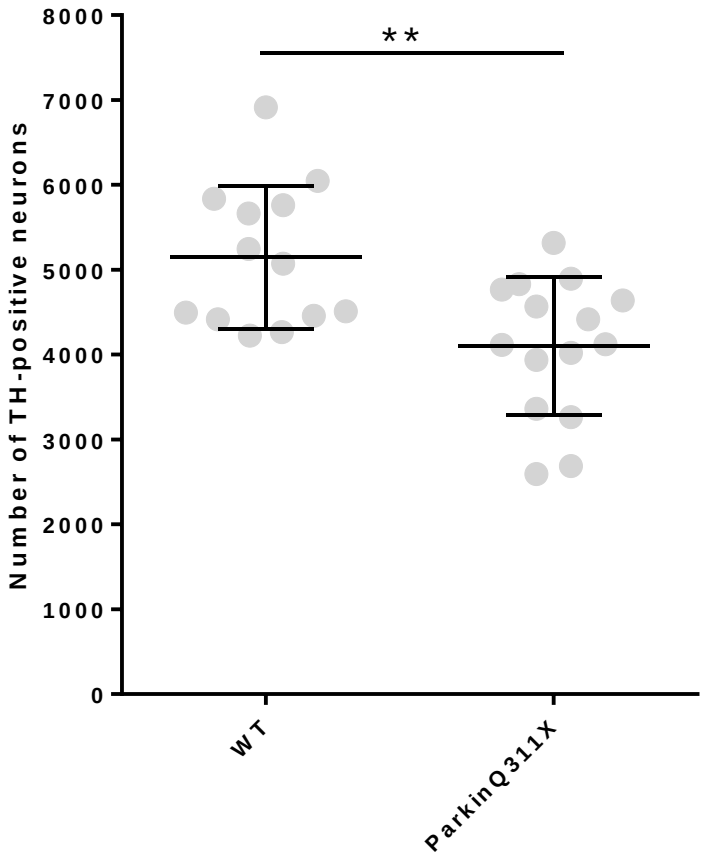

Figure 8. Early degeneration of SNc DA neuron in Parkin-Q311X mice. Histograms showing DA neuron quantification performed by stereology. Data derive from 15 ParkinQ311X mice and 13 WT mice (Student's t-test, unpaired two tailed **p<0.01 different from WT).

4.2. KAR is expressed in SNc DA neurons

Previous data suggested that KAR is expressed in the midbrain [25]. To confirm that KAR is expressed in the SNc DA neurons, we analyzed by western blot the levels of the GluK2/3 KAR subunits in different tissues of wild-type mice. The results showed that GluK2/3 are expressed in various brain areas including midbrain (**Figure 9**).

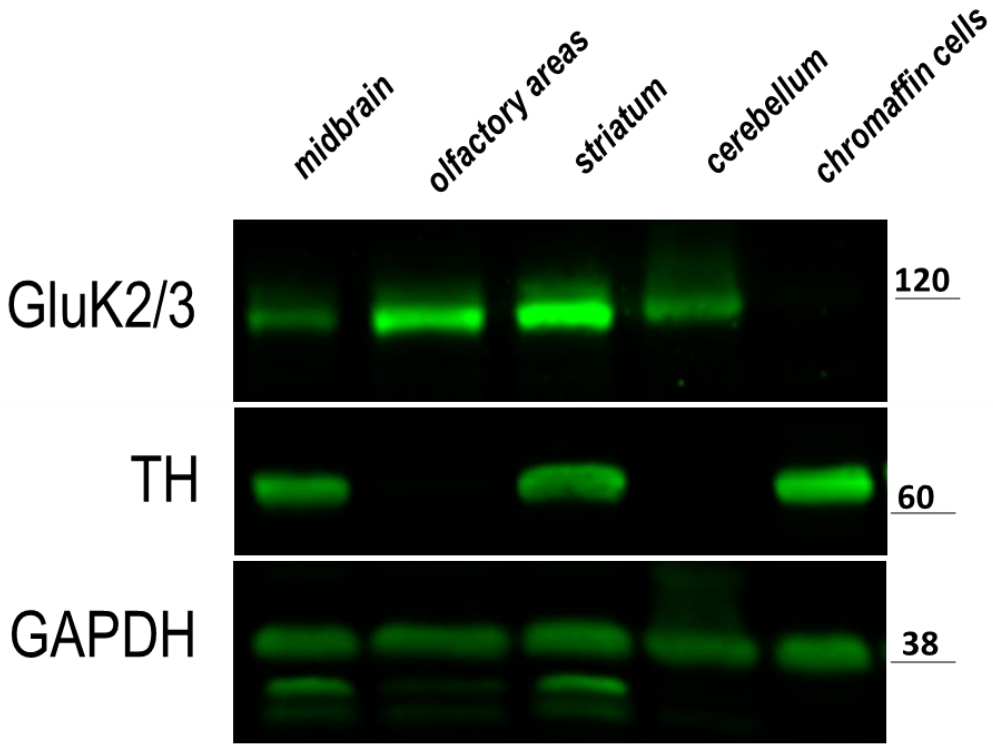

Figure 9. Representative western blots showing that the GluK2 KAR subunit is expressed in various brain areas including midbrain. TH signal is positive in the midbrain and striatum. Chromaffin cells are included in the experiment as a negative control. GAPDH signal confirms equal protein loading.

To further confirm KAR expression in the DA neurons of SNc, we analyzed by immunohistochemistry the levels of the GluK2/3 KAR subunits in wild-type mice. DA neurons were identified by co-labeling with antibody against TH. The results show that a subset of DA neurons are immunoreactive for GluK2/3 (**Figure 10**). This finding shows that DA neurons of SNc express GluK2/3 subunits and suggests that KARs have a role in the regulation DA neuron function.

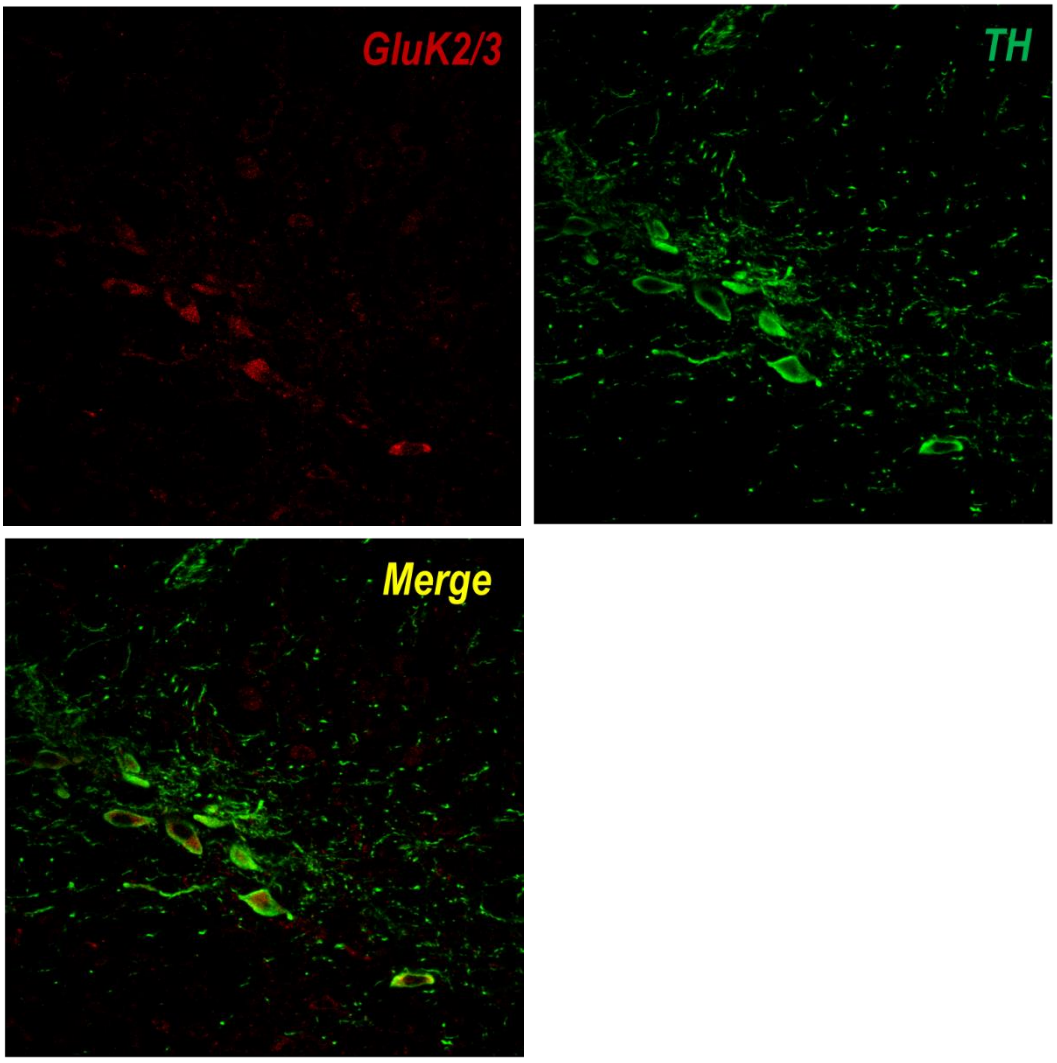

Figure 10. Coronal sections of adult mouse SNc labeled with GluK2/3 antibody (red fluorescence) and TH antibody (green fluorescence). Immunohistochemistry analyses showed that a subset of DA neurons are immunoreactive for GluK2/3.

4.3. The early firing dysfunction of SNc DA neurons in parkinQ311X mice depends on abnormal KAR activation

Here we tested the hypothesis that the early dysfunction of SNc DA neuron firing in parkinQ311X mice depends on abnormal KAR activation. We therefore investigated whether the genetic deletion of the key KAR subunit GluK2 normalizes the firing activity of DA neurons in slices. We crossed parkinQ311X mice with GluK2$^{-/-}$ mice (both on C57BL/6) to generate the following cohorts of mice: parkinQ311X/GluK2$^{-/-}$, parkinQ311X/GluK2$^{+/-}$, parkinQ311X/GluK2$^{+/+}$, GluK2$^{-/-}$, GluK2$^{+/-}$ littermates and WT mice. Genotyping was performed as described[51,53]. We performed a cell-attached and whole-cell patch clamp recordings in DA neurons of the SNc in 25 days-old mouse brain slices to analyze spontaneous firing frequencies and intrinsic membrane parameters (e.g., action potential amplitude, threshold). The results of these experiments are reported in **figure 11**. These results confirm that mutant parkin expression increases AP frequency in SNc DA neurons. Importantly, these experiments also show that full genetic deletion of GluK2 rescues the abnormal firing rate caused by mutant parkin expression. The partial GluK2 deletion (ParkinQ311X-GluK2$^{+/-}$ mice) also decreases the AP frequency, but the difference does not reach statistical significance.

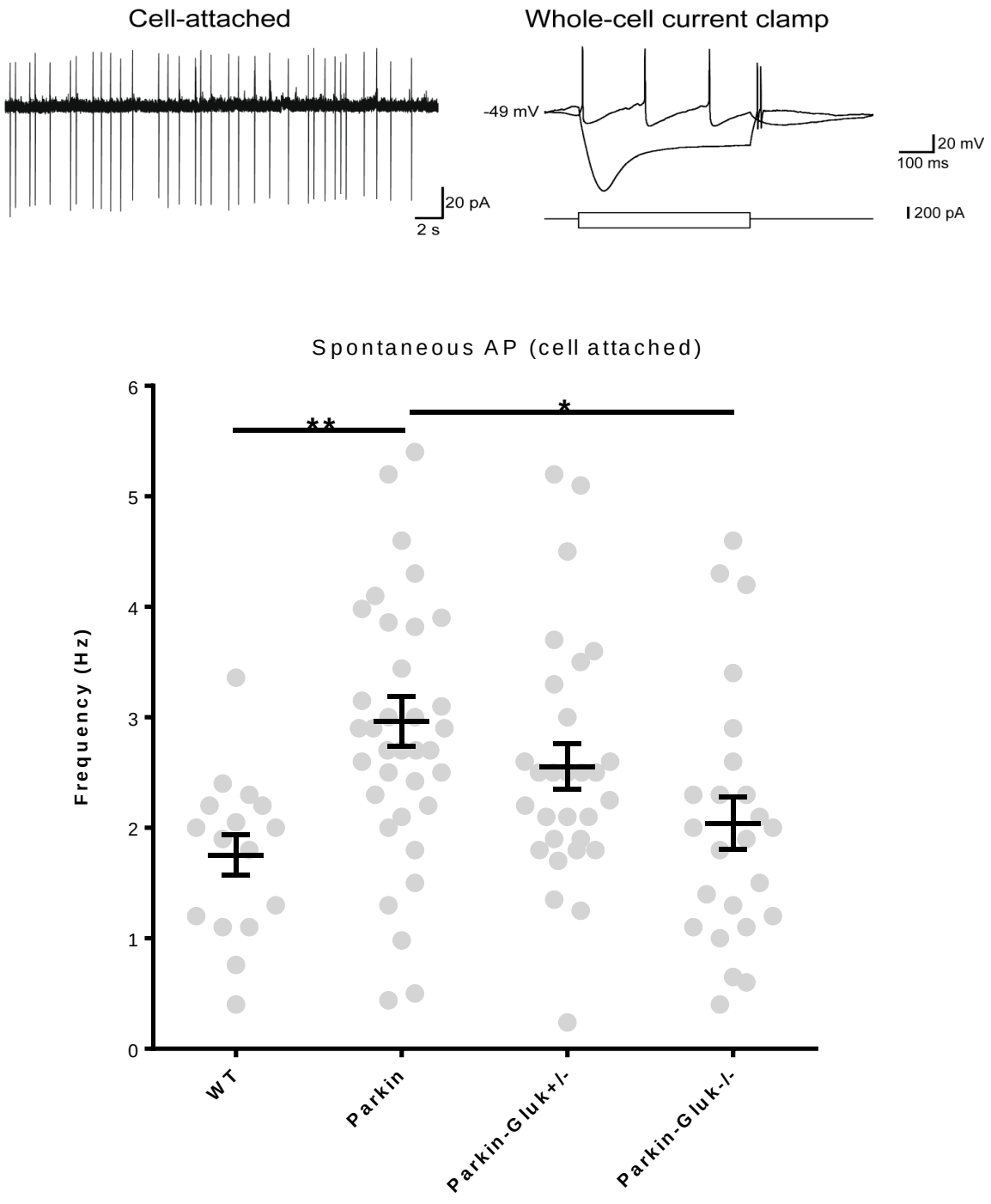

Figure 11. Recordings of the spontaneous firing activity of SNc DA neurons in acute slices of ventral midbrain prepared from mice at 25 days of age. The upper panel shows representative cell-attached and whole-cell patch clamp recordings in DA neurons of the SNc in mouse brain slices. The lower panel shows the quantification of the frequency. Spontaneous firing frequency of SNc DA neurons was increased in ParkinQ311X mice compared to WT mice, and full GluK2 deletion rescues the abnormal firing frequency. Data derive from 8 ParkinQ311X mice (36 recorded neurons), 2 parkinQ311X/GluK2$^{-/-}$ (24 recorded neurons), 4 parkinQ311X/GluK2$^{-/+}$ (29 recorded neurons) and 6 WT mice (16 recorded neurons) (One-way ANOVA followed by the Tukey test *p<0.05; **p<0.001).

Next we tested the hypothesis that genetic GluK2 modulation has neuroprotective effects on the DA neurons of parkinQ311X mice. We crossed parkinQ311X mice with GluK2$^{-/-}$ mice (both on C57BL/6) to generate the following cohorts of mice: parkinQ311X/GluK2$^{-/-}$, parkinQ311X/GluK2$^{+/-}$, parkinQ311X/GluK2$^{+/+}$, GluK2$^{-/-}$ and GluK2$^{+/-}$ littermates, and WT mice. Stereological cell count in SNc and analysis of TH density in striatum were performed on tissue derived from 1-month-old and 6-month-old mice, according to standard protocols[55,56]. Results of stereological cell count in SNc are reported in **figure 12**. No statistically significant differences were found among mice cohorts at 1 month of age. This data is in agreement with the previous paper showing that DA neuron death in ParkinQ311X mice is undetectable at 1 month of age[51]. This result also suggests that GluK2 deletion does not induce developmental changes in DA neuron of SNc.

ParkinQ311X mice show a reduced number of DA neurons in SNc as compared to WT littermates at 6 months of age. This result confirms that this parkin mouse displays the main neuropathological feature of ARJP, i.e. the loss of DA neurons. A slightly greater number of DA neurons can be observed in parkinQ311X/GluK2$^{-/-}$ and parkinQ311X/GluK2$^{+/-}$ mice as compared to parkinQ311X mice, but this difference is not statistically significant. Thus, in our mice cohorts, GluK2 genetic deletion does not rescue DA neuron survival in ParkinQ311X mice. Moreover, no differences in striatal TH optical density were found among different genotypes (data not shown).

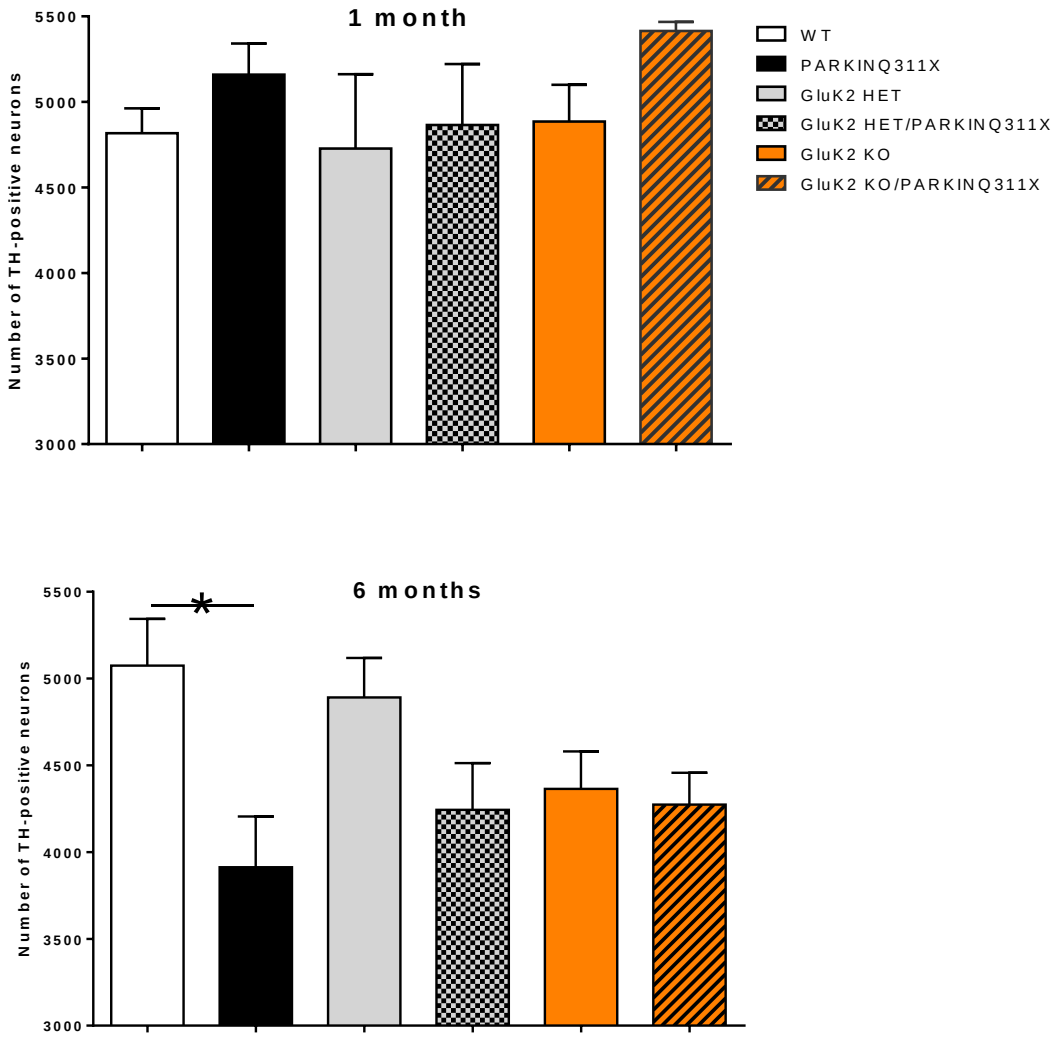

Figure 12. Histograms showing DA neuron quantification performed by stereological count. Data derive from 2 parkinQ311X/GluK2$^{-/-}$, 10 parkinQ311X/GluK2$^{-/+}$, 10 parkinQ311X/GluK2$^{+/+}$, 7 GluK2$^{-/-}$ and 10 GluK2$^{+/-}$ littermates, and 10 wild-type mice at 1 month of age and from 7 parkinQ311X/GluK2$^{-/-}$, 11 parkinQ311X/GluK2$^{-/+}$, 11 parkinQ311X/GluK2$^{+/+}$, 10 GluK2$^{-/-}$ and 12 GluK2$^{+/-}$ littermates, and 11 wild-type mice at 6 months of age (One-way ANOVA followed by the Tukey test *p<0.05).

4.4. The KAR antagonist UBP310 prevents the loss of SNc DA neurons in parkinQ311X mice

Here we tested the hypothesis that pharmacological KAR modulation can have neuroprotective effects on the DA neurons of parkinQ311X mice. First, we performed a preliminary pharmacokinetic study of UBP310 in order to confirm that this molecule is able to cross the blood-brain barrier. We treated WT mice with 20mg/Kg i.p. UBP310 and then performed a time-course analysis of UBP310 levels in the brain at 10min, 30min, 1h, 2h, 4h, 8h and 24hafter administration. Our results show that UBP310 is quickly distributed to the brain after i.p. injection, and 24h after injection, the substance is still detectable in brain tissue (**Figure 13**).

a

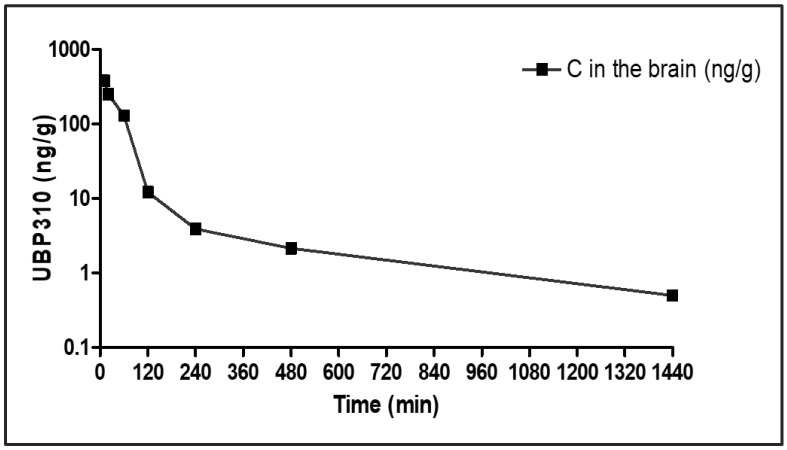

b

Time (min)	Calculated concentration in the brain (ng/g)
10	379.5
30	251.5
60	129.8
120	12.2
240	3.9
480	2.14
1440	0.5

c

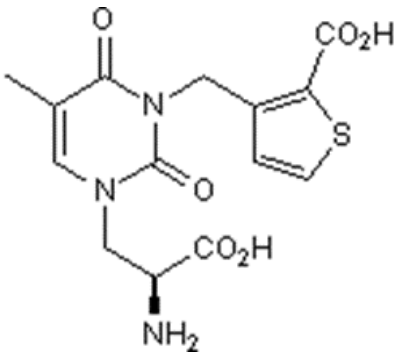

Figure 13. Graph (a) and table (b) showing the concentration of UBP310 in mouse brain at different times after the administration. Each time-point is the mean of 2 mice. The structure of UBP310 molecule is shown in panel C.

Next, we performed a dose-response curve of UBP310 in WT mice to calculate the ED_{50}, namely the dose of UBP310 able to decrease SNc DA firing activity by 50%. We performed an in-vivo single-unit extracellular recording of SNc DA neurons and analysed the effects of cumulative doses of UBP310 (10-60mg/Kg, i.p.) on SNc DA firing activity. The resulting ED_{50} is 13 mg/Kg, while the dose that decreases the firing rate by ~75% is 20mg/Kg (**Figure 14**).

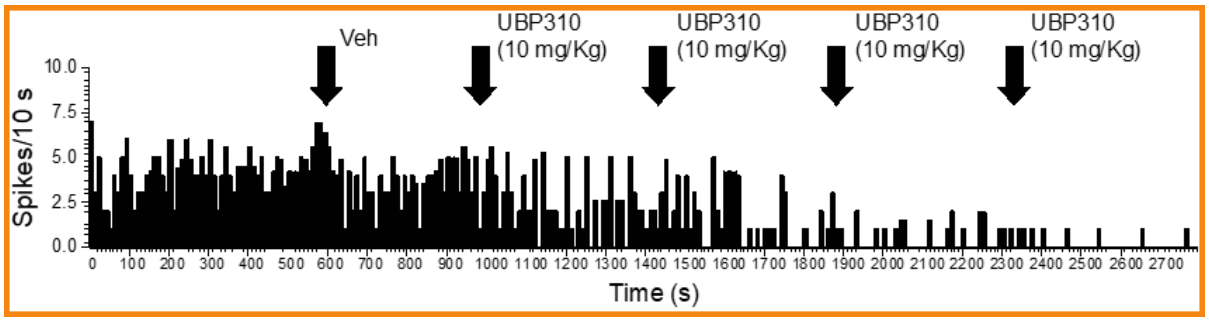

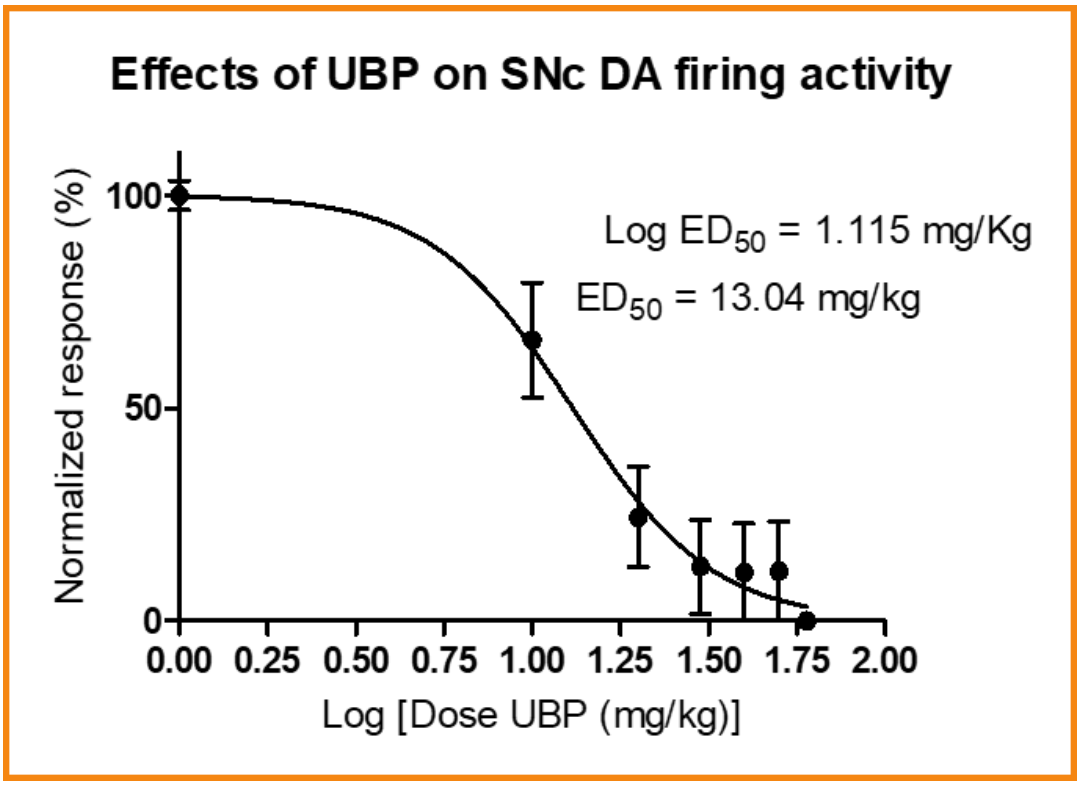

Figure 14. The firing activity of SNc DA neurons was analyzed by in-vivo single-unit extracellular recording in 3-month-old wild-type mice upon intraperitoneal (i.p.) injection of UBP310 (10-60 mg/kg). The upper panel shows the representative integrated firing rate histograms. The lower panel shows that UBP310 (10-40 mg/kg, i.p.) dose-dependently reduces the firing activity of SNc DA neurons in WT mice. 13mg/Kg is the UBP310 dose that decreases the firing rate by 50% (ED_{50}), 20mg/Kg is the dose that decreases the firing rate by ~75%.

Then we tested the hypothesis that UBP310 increases DA neuronal survival in parkinQ311X mice. Because electrophysiological experiments (**Figure 11**) suggested that the deletion of 50% of GluK2 was not sufficient to reach a full rescue of normal firing activity of DA neurons, we decided to treat the animal with UBP310 dose higher than the ED_{50}, i.e. 20mg/Kg, that is the dose that decreases the firing rate by ~75%.

Three-month-old parkinQ311X mice and WT littermates were treated daily with UBP310 (20mg/kg, i.p) or vehicle (10% DMSO in saline, i.p.) for 90 days.

As the chronic treatment progressed, we realized that neither vehicle nor UBP310 cause toxicity. We found no evidence of mortality or weight change (**Figure 15**), no signs of acute pain or distress or toxicity, animals were able to eat, walk, groom normally. Therefore, we added a second experimental group. Starting from 1.5 months of age, 9 ParkinQ311X mice were treated daily with UBP310 (20mg/kg/day, i.p.) for 135 days. At the end of treatments, animals were sacrificed by perfusion and stereological cell count in SNc was performed as described in Materials and Methods section. Data are shown in **figure 16**. We found that UBP310 treatment for 135 days rescues DA neurons from death caused by parkinQ311X expression. ANOVA did not reveal a significant rescue effect in mice treated for 90 days with UBP310. Nonetheless, they appear to be protected if compared with ParkinQ311X mice treated with vehicle if an unpaired Student's t-test (with Welch's correction) is performed (p=0.016). The different statistical outcome may be due to the overall variability, and calls for an increase in the number of animals in this experimental group.

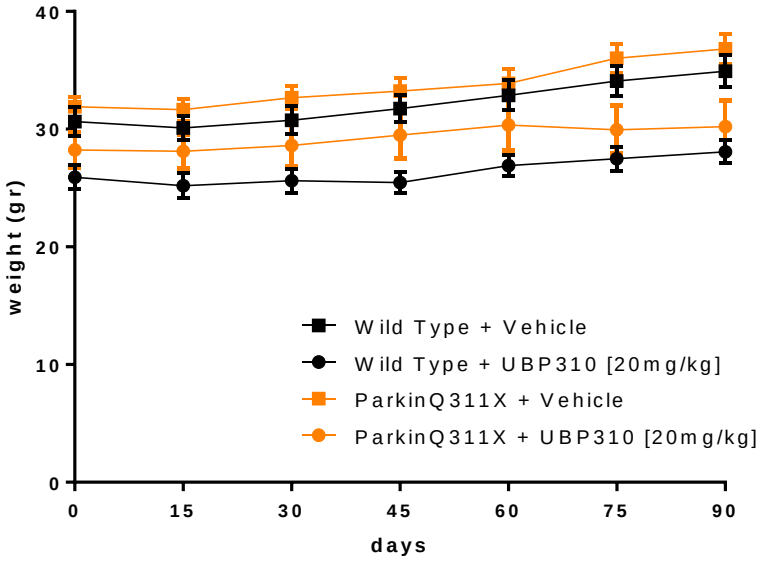

Figure 15. Graph showing the weight of the animals during the 3 months of treatment. The weights were checked every 15 days.

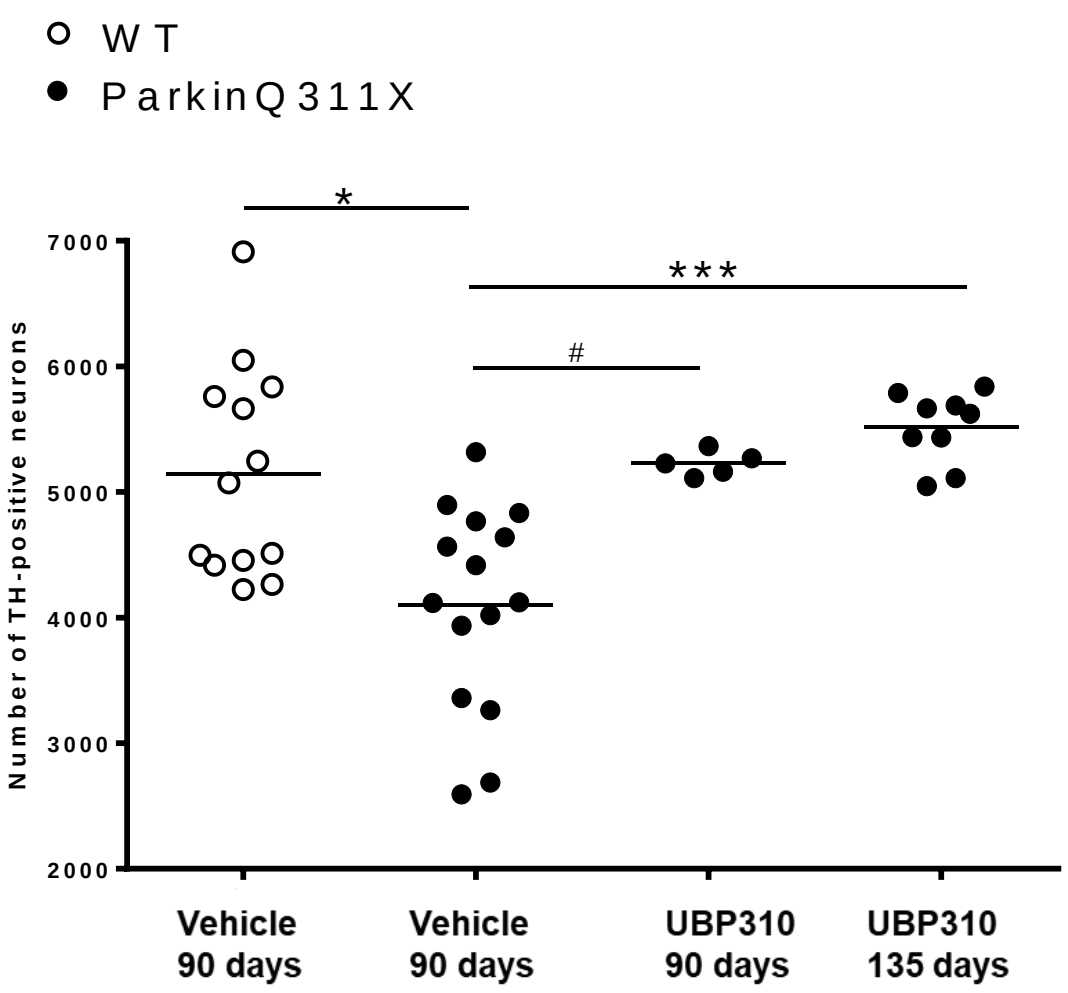

Figure 16. Dot plot showing DA neuron quantification performed by stereological count in WT and parkinQ311X mice treated with vehicle or UBP310. Data are mean ± SEM. Parkin-Q311X mice treated with vehicle (n=15) showed degeneration of SNc DA neuron as compared to WT mice treated with vehicle (n=12) (Kruskal-Wallis test followed by Dunn's multiple comparisons test, *p<0.05). UBP310 treatment for 135 days (n=9 parkinQ311X mice) rescues DA neurons from death caused by parkinQ311X expression (Kruskal-Wallis test followed by Dunn's multiple comparisons test, ***p<0.001 vs WT mice treated with vehicle). Student's t-test with Welch's correction reveal a significant rescue effect in mice treated for 90 days with UBP310 (n=5 parkinQ311X mice treated with UBP310 vs parkinQ311X mice treated with vehicle, #p=0.016).

DISCUSSION

5. DISCUSSION

Our previous study showed that parkin interacts with and ubiquitinates the GluK2 KAR subunit and regulates GluK2 levels and KAR currents[38]. We found that GluK2 interacts with Ubl-linker domain of parkin, similar to other parkin substrates[57]. We also found that the loss of parkin function or the expression of parkin mutants associated with ARJP lead to GluK2/KAR accumulation and increased postsynaptic KAR currents in neurons[38]. Because KARs regulate neuron excitability[27,58], we hypothesized that KARs accumulation at the post-synapse of ARJP DA neurons can dysregulate DA neuron excitability.

Thus, we decided to test the hypothesis that the partial or total block of KAR rescues abnormal DA neuron excitability in the parkinQ311X mouse model. Data from this project confirm the preliminary findings that the spontaneous firing frequency of ParkinQ311X-DA neurons is increased as compared to WT DA neurons. The spontaneous activity pattern of adult SNc DA neurons results from the interactions between intrinsic and synaptic currents. In adult SNc DA neurons, low-frequency tonic background activity is generated by intrinsic pacemaker mechanisms, whereas burst generation depends on intact synaptic inputs in particular the glutamatergic ones. Because, according to the literature, only the pacemaker-like pattern can be recorded in vitro[59,60], our data suggest that the expression of parkin mutants in SNc DA neurons affect their pacemaker activity.

This data is in agreement with a previous study that investigated the firing frequency of DA neurons in a different PD model, generated by overexpressing mutant α-synuclein[61], overall suggesting that an increase in the spontaneous firing of DA neurons may be a common feature in PD forms caused by different pathogenic stimuli.

Our electrophysiological experiments show that the full genetic deletion of GluK2 rescues the abnormal firing rate in DA neurons caused by mutant parkin expression. This result confirms the hypothesis that early dysregulation of SNc DA neuron depends on the increased KAR activity. This result also supports the hypothesis that GluK2 is a potential target in order to normalize the firing frequency of DA neurons in ARJP. What is the mechanism by which KAR receptor could

regulate spontaneous firing in DA neurons? Pacemaker activity is associated with dopamine release and it is intrinsically driven by the L-type voltage gated calcium channel (L-VGCC) Cav1.3. We can hypothesize that through the gating of the channel (canonical pathway) KAR can facilitate membrane depolarization. On the other hand, because KARs activate G proteins signaling through the stimulation of phospholipase C and PKC (non canonical pathway) we can hypothesize that KAR activation induces post-translational modifications of the Cav1.3.

Because of their large fractional calcium influx during action potential firing and their enormously large axonal tree, SNc DA neurons constitutively carry a higher metabolic demand compared with other neurons[62]. Thus, by increasing KAR-mediated glutamatergic transmission and changing pacemaker activity, *PARK2* mutations can lead to early dysregulation of electrical activity of SNc DA neurons, altered calcium influx, thereby increasing their energy costs and susceptibility to oxidative damage, calcium overload and excitotoxicity.

Our results confirm that the expression of the mutant parkin variant Q311X *in vivo* induces the degeneration of SNc DA neurons, although we were not able to demonstrate that the partial or total GluK2 deletion does not induce a statistically significant rescue of DA neuron viability. Yet unidentified mechanisms may underlie this lack of neuroprotection.

To further investigate the role of KAR as a potential target for neuroprotection in ARJP, we tested the potential neuroprotective effects of the GluK2/GluK5 antagonist UBP310[63,64]. We found that UBP310 is able to cross the blood brain barrier, that UBP310 is quickly distributed to the brain after i.p. injection, and that 24h after the injection the substance is still detectable in the brain. These results are consistent with a previous finding that i.p. administration of UBP310 results in central effects including protection from kainate induced seizures[64]. According to our results, 3-month and 4.5-month treatment with UBP310 (20 mg/kg/day i.p.) does not induce any apparent toxicity to WT and Q311X mice. UBP310 treatment rescues DA neuron degeneration caused by parkinQ311X expression. This result strongly supports the potential role of KAR as target for neuroprotective therapy in ARJP. It remains to be investigated if UBP310, in addition to preventing the degeneration of DA neurons, is also able to prevent the development of PD-like motor impairment. To accomplish this aim, it will be necessary to test this drug in an ARJP mouse model that shows motor deficits in addition to nigrostriatal

degeneration. Moreover it will be important to test this drug in human cells derived from ARJP patients. Non-neuronal cells such as fibroblasts from parkin patients are hardly usable because they do not have functional KAR expression. An interesting possibility is testing this drug on dopaminergic neurons derived from induced pluripotent stem cells (IPSC) prepared from ARJP patients. However, it has been reported that the expression of glutamate receptors in neurons derived from IPSC is not equal to that typical of mature neurons, so before proceeding with this step it will be important to check if DA neurons derived from IPSC express functional KAR. Furthermore, it will be important to test whether this molecule that shows a neuroprotective effect on dopaminergic neurons, is also effective in other forms of parkinsonism that have a higher frequency in the population. It will be also important to investigate the benefit-toxicity profile of this molecule in order to understand if it can cause toxic effects in other neuronal systems, and to prove that other KAR antagonists are effective in ARJP and other parkinsonism forms.

In conclusion, our data reveal a novel aspect of parkin neurobiology, i.e. the control over synaptic function, which adds to the current scientific scenario that views parkin as a key regulator of the mitochondrial function, a role accomplished via ubiquitination of the proteins of the mitochondrial outer membrane and regulation of mitochondria turnover[65].

It is difficult to speculate about the possibility that KAR hyperactivation is responsible for mitochondria dysfunction in *PARK2* models because, based on the current literature, these two pathways do not directly connect and seem related to two different functions of parkin. However, a reciprocal influence between alteration of mitochondrial functionality and synaptic activity has been extensively reported[66–68], so it conceivable that a synaptic alteration, such as overactivity of the KAR receptor, may precipitate a pre-existing and concomitant mitochondrial damage.

Although further studies are needed to ascertain whether mitochondrial impairment and synaptic dysfunction induced by loss of parkin in DA neurons are separate events or related phenomena, we can hypothesize that the loss of this dual control of parkin over both mitochondrial and synaptic function can contribute to the vulnerability of DA SNc neurons in *PARK2*-related PD.

BIBLIOGRAPHY

6. BIBLIOGRAPHY

1. Kasten, M. *et al.* Genotype-phenotype relations for the Parkinson's Disease genes Parkin, PINK1, DJ1: MDSGene Systematic Review. *Mov. Disord.* **33,** 730–741 (2018).
2. Kasten, M., Marras, C. & Klein, C. Nonmotor Signs in Genetic Forms of Parkinson's Disease. in *International Review of Neurobiology* 129–156 (2017). doi:10.1016/bs.irn.2017.05.030
3. Khan, N. L. *et al.* Parkin disease: A phenotypic study of a large case series. *Brain* **126,** 1279–1292 (2003).
4. Paviour, D. C., Surtees, R. A. H. & Lees, A. J. Diagnostics considerations in juvenile parkinsonism. *Mov. Disord.* **19,** 123–135 (2004).
5. Schrag, A. & Schott, J. M. Epidemiological, clinical, and genetic characteristics of early-onset parkinsonism. *Lancet Neurology* **5,** 355–363 (2006).
6. Grünewald, A., Kasten, M., Ziegler, A. & Klein, C. Next-generation phenotyping using the Parkin example: Time to catch up with genetics. *JAMA Neurol.* **70,** 1186–1191 (2013).
7. Mitsuyama, S., Ohtsubo, M., Minoshima, S. & Shimizu, N. D ATABASE IN B RIEF The KM-parkin-DB : A Sub-set MutationView Database Specialized for PARK2 (PARKIN) Variants. **2440,** 2430–2440 (2015).
8. Kitada, T. *et al.* Mutations in the parkin gene cause autosomal recessive juvenile parkinsonism. *Nature* **392,** 605–608 (1998).
9. Poulopoulos, M., Levy, O. A. & Alcalay, R. N. The neuropathology of genetic Parkinson's disease. *Movement Disorders* **27,** 831–842 (2012).
10. Sunada, Y., Saito, F., Matsumura, K. & Shimizu, T. Differential expression of the parkin gene in the human brain and peripheral leukocytes. *Neurosci.Lett.* **254,** 180–182 (1998).
11. Serdaroglu, P., Hanagasi, H., Tasli, H. & Emre, M. Parkin expression in muscle from three patients with autosomal recessive Parkinson's disease carrying parkin mutation. *Acta Myol.* **24,** 2–5 (2005).
12. Fujiwara, M. *et al.* Parkin as a tumor suppressor gene for hepatocellular carcinoma. *Oncogene* **27,** 6002–6011 (2008).

13. Auburger, G. *et al.* Primary skin fibroblasts as a model of Parkinson's disease. *Mol. Neurobiol.* **46,** 20–27 (2012).
14. Kasap, M., Akpinar, G., Sazci, A., Idrisoglu, H. A. & Vahaboğlu, H. Evidence for the presence of full-length PARK2 mRNA and Parkin protein in human blood. *Neurosci. Lett.* **460,** 196–200 (2009).
15. Picchio, M. C. *et al.* Alterations of the tumor suppressor gene Parkin in non-small cell lung cancer. *Clin Cancer Res* **10,** 2720–2724 (2004).
16. Cookson, M. R. Parkin's Substrates and the Pathways Leading to Neuronal Damage Genetic Loci in Familial Parkinson's Disease. *NeuroMolecular Med.* **3,** 1–13 (2003).
17. Zhang, C.-W., Hang, L., Yao, T.-P. & Lim, K.-L. Parkin Regulation and Neurodegenerative Disorders. *Front Aging Neurosci.* **7,** (2015).
18. Houlden, H. & Singleton, A. B. The genetics and neuropathology of Parkinson's disease. *Acta Neuropathologica* **124,** 325–338 (2012).
19. Scarffe, L. a., Stevens, D. a., Dawson, V. L. & Dawson, T. M. Parkin and PINK1: Much more than mitophagy. *Trends Neurosci.* **37,** 315–324 (2014).
20. Charan, R. A. & LaVoie, M. J. Pathologic and therapeutic implications for the cell biology of parkin. *Mol. Cell. Neurosci.* **66,** 62–71 (2015).
21. Seirafi, M., Kozlov, G. & Gehring, K. Parkin structure and function. *FEBS Journal* 2076–2088 (2015). doi:10.1111/febs.13249
22. Coussen, F. Molecular determinants of kainate receptor trafficking. *Neuroscience* (2009). doi:10.1016/j.neuroscience.2007.12.052
23. Jaskolski, F., Coussen, F. & Mulle, C. Subcellular localization and trafficking of kainate receptors. *Trends in Pharmacological Sciences* (2005). doi:10.1016/j.tips.2004.11.008
24. Jaskolski, F. Subunit Composition and Alternative Splicing Regulate Membrane Delivery of Kainate Receptors. *J. Neurosci.* (2004). doi:10.1523/JNEUROSCI.5116-03.2004
25. Porter, R. H. P., Eastwood, S. L. & Harrison, P. J. Distribution of kainate receptor subunit mRNAs in human hippocampus, neocortex and cerebellum, and bilateral reduction of hippocampal GluR6 and KA2 transcripts in schizophrenia. *Brain Res.* (1997). doi:10.1016/S0006-8993(96)01404-7

26. Mueller, H. T., Haroutunian, V., Davis, K. L. & Meador-Woodruff, J. H. Expression of the ionotropic glutamate receptor subunits and NMDA receptor-associated intracellular proteins in the substantia nigra in schizophrenia. *Mol. Brain Res.* (2004). doi:10.1016/j.molbrainres.2003.11.004
27. Lerma, J. & Marques, J. M. Kainate receptors in health and disease. *Neuron* (2013). doi:10.1016/j.neuron.2013.09.045
28. Lerma, J. Kainate Receptor Functions. in *Encyclopedia of Neuroscience* (2010). doi:10.1016/B978-008045046-9.01215-8
29. Helton, T. D., Otsuka, T., Lee, M., Mu, Y. & Ehlers, M. D. Pruning and loss of excitatory synapses by the parkin ubiquitin ligase. (2008).
30. Kubo, S. *et al.* Parkin is associated with cellular vesicles. 42–54 (2001).
31. Huttner, W. B., Schiebler, W., Greengard, P. & De Camilli, P. Synapsin I (protein I), a nerve terminal-specific phosphoprotein. III. Its association with synaptic vesicles studied in a highly purified synaptic vesicle preparation. *J. Cell Biol.* **96,** 1374–1388 (1983).
32. Mouatt-Prigent, A. *et al.* Ultrastructural localization of parkin in the rat brainstem, thalamus and basal ganglia. *J. Neural Transm.* **111,** 1209–1218 (2004).
33. Fallon, L. *et al.* Parkin and CASK / LIN-2 Associate via a PDZ-mediated Interaction and Are Co-localized in Lipid Rafts and Postsynaptic Densities in Brain *. **277,** 486–491 (2002).
34. Sheng, M. & Kim, E. The postsynaptic organization of synapses. *Cold Spring Harb. Perspect. Biol.* **3,** (2011).
35. Ye, F. & Zhang, M. Structures and target recognition modes of PDZ domains: recurring themes and emerging pictures. *Biochem. J.* **455,** 1–14 (2013).
36. Hsueh, Y. P. Calcium/calmodulin-dependent serine protein kinase and mental retardation. *Annals of Neurology* **66,** 438–443 (2009).
37. Joch, M. *et al.* Parkin-mediated Monoubiquitination of the PDZ Protein PICK1 Regulates the Activity of Acid-sensing Ion Channels. **18,** 3105–3118 (2007).
38. Maraschi, A. *et al.* Parkin regulates kainate receptors by interacting with the GluK2 subunit. *Nat. Commun.* **5,** 5182 (2014).

39. Cremer, J. N. *et al.* Changes in the expression of neurotransmitter receptors in Parkin and DJ-1 knockout mice - A quantitative multireceptor study. *Neuroscience* **311,** 539–551 (2015).
40. Yetnikoff, L., Lavezzi, H. N., Reichard, R. A. & Zahm, D. S. An update on the connections of the ventral mesencephalic dopaminergic complex. *Neuroscience* **282,** 23–48 (2014).
41. Ambrosi, G., Cerri, S. & Blandini, F. A further update on the role of excitotoxicity in the pathogenesis of Parkinson???s disease. *J. Neural Transm.* **121,** 849–859 (2014).
42. Mehta, A., Prabhakar, M., Kumar, P., Deshmukh, R. & Sharma, P. L. Excitotoxicity: Bridge to various triggers in neurodegenerative disorders. *European Journal of Pharmacology* **698,** 6–18 (2013).
43. Lozano, A. M., Dostrovsky, J., Chen, R. & Ashby, P. Deep brain stimulation for Parkinson's disease: disrupting the disruption. *Lancet Neurol.* **1,** 225–231 (2002).
44. Schapira, A. H. & Jenner, P. Etiology and pathogenesis of Parkinson's disease. *Movement Disorders* **26,** 1049–1055 (2011).
45. Olanow, C. W. & Tatton, W. G. Etiology and pathogenesis of Parkinson's disease. *Annu. Rev. Neurosci.* **22,** 123–144 (1999).
46. Castillo, J. Del & Katz, B. Quantal components of the end-plate potential. *J. Physiol.* **124,** 560–573 (1954).
47. Katz, B. Quantal mechanism of neural transmitter release. in *Nobel Lectures, Physiology or Medicine 1963-1970* **173,** 485–492 (1970).
48. Mereu, G., Costa, E., Armstrong, D. M. & Vicini, S. Glutamate receptor subtypes mediate excitatory synaptic currents of dopamine neurons in midbrain slices. *J Neurosci* **11,** 1359–1366 (1991).
49. Staropoli, J. F. *et al.* Parkin Is a Component of an SCF-like Ubiquitin Ligase Complex and Protects Postmitotic Neurons from Kainate Excitotoxicity. *Neuron* **37,** 735–749 (2003).
50. Rodriguez, M. C., Obeso, J. A. & Olanow, C. W. Subthalamic nucleus-mediated excitotoxicity in Parkinson's disease: a target for neuroprotection. *Ann. Neurol.* **44,** S175-88 (1998).
51. Lu, X.-H. *et al.* Bacterial artificial chromosome transgenic mice expressing a truncated mutant parkin exhibit age-dependent hypokinetic motor

deficits, dopaminergic neuron degeneration, and accumulation of proteinase K-resistant alpha-synuclein. *J. Neurosci.* **29,** 1962–76 (2009).

52. Hattori, N. *et al.* Point Mutations (Thr240Arg and Ala311Stop) in the Parkin Gene. **758,** 754–758 (1998).
53. Mulle, C. *et al.* Altered synaptic physiology and reduced susceptibility to kainate- induced secures in GluR6-deficient mice. *Nature* (1998). doi:10.1038/33408
54. Paxinos, G., Franklin, K. B. J., Paxinos, G and Franklin, K. B. J., Paxinos, G. & Franklin, K. B. J. *Mouse Brain in Stereotaxic Coordinates*. *Academic Press* (2001). doi:10.1016/S0306-4530(03)00088-X
55. Novello, S. *et al.* G2019S LRRK2 mutation facilitates α-synuclein neuropathology in aged mice. *Neurobiol. Dis.* (2018). doi:10.1016/j.nbd.2018.08.018
56. Arcuri, L. *et al.* Genetic and pharmacological evidence that endogenous nociceptin/orphanin FQ contributes to dopamine cell loss in Parkinson's disease. *Neurobiol. Dis.* **89,** 55–64 (2016).
57. Spratt, D. E., Walden, H. & Shaw, G. S. RBR E3 ubiquitin ligases: new structures, new insights, new questions. *Biochem. J.* (2014). doi:10.1042/BJ20140006
58. Contractor, A., Mulle, C. & Swanson, G. T. Kainate receptors coming of age: Milestones of two decades of research. *Trends in Neurosciences* (2011). doi:10.1016/j.tins.2010.12.002
59. Richards, C. D., Shiroyama, T. & Kitai, S. T. Electrophysiological and immunocytochemical characterization of GABA and dopamine neurons in the substantia nigra of the rat. *Neuroscience* (1997). doi:10.1016/S0306-4522(97)00093-6
60. Paladini, C. A. & Roeper, J. Generating bursts (and pauses) in the dopamine midbrain neurons. *Neuroscience* (2014). doi:10.1016/j.neuroscience.2014.07.032
61. Subramaniam, M. *et al.* Mutant -Synuclein Enhances Firing Frequencies in Dopamine Substantia Nigra Neurons by Oxidative Impairment of A-Type Potassium Channels. *J. Neurosci.* (2014). doi:10.1523/JNEUROSCI.5069-13.2014
62. Bolam, J. P. & Pissadaki, E. K. Living on the edge with too many mouths

to feed: Why dopamine neurons die. *Mov. Disord.* (2012). doi:10.1002/mds.25135

63. Pinheiro, P. S. *et al.* Selective block of postsynaptic kainate receptors reveals their function at hippocampal mossy fiber synapses. *Cereb. Cortex* (2013). doi:10.1093/cercor/bhs022
64. Peret, A. *et al.* Contribution of Aberrant GluK2-Containing Kainate Receptors to Chronic Seizures in Temporal Lobe Epilepsy. *Cell Rep.* (2014). doi:10.1016/j.celrep.2014.06.032
65. Pickrell, A. M. & Youle, R. J. The roles of PINK1, Parkin, and mitochondrial fidelity in parkinson's disease. *Neuron* (2015). doi:10.1016/j.neuron.2014.12.007
66. Sheng, Z. H. & Cai, Q. Mitochondrial transport in neurons: Impact on synaptic homeostasis and neurodegeneration. *Nature Reviews Neuroscience* (2012). doi:10.1038/nrn3156
67. Li, Z., Okamoto, K. I., Hayashi, Y. & Sheng, M. The importance of dendritic mitochondria in the morphogenesis and plasticity of spines and synapses. *Cell* **119,** 873–887 (2004).
68. Lee, A., Hirabayashi, Y., Kwon, S. K., Lewis, T. L. & Polleux, F. Emerging roles of mitochondria in synaptic transmission and neurodegeneration. *Current Opinion in Physiology* (2018). doi:10.1016/j.cophys.2018.03.009